Received xx April xxxx; | Revised xx June xxxx; | Accepted xx June xxxx
DOI: xxx/xxxx

ARTICLE TYPE

Rational Solutions of Multi-component Nonlinear Schrödinger Equation and Complex Modified KdV Equation

Lihong Wang[1,2] | Jingsong He*[3] | Róbert Erdélyi[2,4]

[1]School of Mathematics and Statistics, Ningbo University, Ningbo 315211, P. R. China
[2]Solar Physics and Space Plasma Research Centre, School of Mathematics and Statistics, University of Sheffield, Hicks Building, Hounsfield Road, Sheffield S3 7RH, United Kingdom
[3]Org Division, Org Name, State name, Country name
[4]Dept of Astronomy, Eötvös University, Pázmány P. sétány 1/A, Budapest, H-1117, Hungary

Correspondence
*Corresponding author, Email: hejingsong@szu.edu.cn; jshe@ustc.edu.cn

Summary

In this paper, the critical condition to achieve rational solutions of the multi-component nonlinear Schrödinger equation is proposed by introducing two nilpotent Lax matrices. Taking the series multisections of the vector eigenfunction as a set of fundamental eigenfunctions,an explicit formula of the nth-order rational solution is obtained by the degenerate Darboux transformation, which is used to generate some new patterns of rogue waves. A conjecture about the degree of the nth-order rogue waves is summarized. This conjecture also holds for rogue waves of the multi-component complex modified Korteweg-de Vries equation. Finally, the semi-rational solutions of the Manakov system are discussed.

KEYWORDS:
Multi-component nonlinear Schrödinger equation Multi-component complex modified KdV equation Rogue wave Darboux transformation Series multisection

1 | INTRODUCTION

In the past 50 years, rogue waves (RWs), known as freak waves or extreme waves, which appear from nowhere and disappear without a trace[1, 2], are regularly observed as giant and devastating waves in the ocean. The height of a RW is at least twice the significant wave height[3, 4]. In recent decades, the concept of RWs has been widely studied beyond oceanic applications, and the phenomena of RWs have been observed in a wide variety of areas of mathematics and physical sciences, including e.g. watertanks[5, 6], Bose-Einstein condensates[7, 8], plasmas[9, 10], nonlinear optics[11–14], and so on.

One of the mathematical models for describing RWs is the rational solutions associated with the focusing nonlinear Schrödinger equation(NLS)[15, 16]. In its dimensionless form, NLS can be written as (each subscripted variable stands for partial differentiation)

$$\mathbf{i}q_t + q_{xx} + 2|q|^2 q = 0, \tag{1}$$

with the form of a (quasi-)rational solution:

$$q(x,t) = \frac{G(x,t)}{F(x,t)} \exp\left(\mathbf{i}(ax + bt)\right).$$

Here, $\mathbf{i}$ denotes the imaginary unit; $q = q(x,t)$ is the wave envelope; t is the temporal variable; x is the spatial variable; F, G are both polynomials in x, t; and real parameters a, b denote the wavenumber and frequency of the progressive wave, respectively. Indeed, the Korteweg-de Vries (KdV) and NLS equations are the prototypes of integrable nonlinear partial differential equations, however, KdV for shallow water wave and NLS for deep water wave. Taking NLS (1) as an example, while the complex spectral parameter λ tends to a certain critical value $\lambda_0 \in \mathbb{C} \setminus \mathbb{R}$, the breather solutions (space-period Akhmediev breather[17] and time-period Kuznetsov-Ma soliton[18, 19]) lead to the ideal Peregrine soliton[20]

$$q(x,t)=\left(\frac{4(1+4\mathbf{i}t)}{1+4x^2+16t^2}-1\right)\mathrm{e}^{2\mathbf{i}t},$$

which is known as the representation of 1st-order RW for its localized nonlinear structure and highly similar profile. The Peregrine soliton above is also obtained by semi-classical approximate expansion of a solution for the NLS at the gradient catastrophe point[21], although there it is called rational breather solution.

This solution is of fundamental significance, because it is doubly localized in both time and space, and defines the limit of a class of breather solutions of the NLS. The mechanism of generating RWs has been presented in e.g. Refs.[22–24]. Recently, it is suggested that the nonlinear stage of modulational instability is a better interior mechanism for RWs[25–28].

The construction of high-order rational (or rogue wave) solutions is one of the important advances in the study of nonlinear waves. In particular, high-order rational solutions have been found by inverse scattering transformation (IST)[26, 29, 30], Hirota bilinear method[31, 32], Darboux transformation (DT) method[33–36], and so forth. For the sake of brevity, in this paper, we use the augmented matrix instead of the ratio of the determinant representation of the DT[37, 38], based on the Cramer's rule.

In addition, a class of rational solutions of several physical systems governed by the complete integrable system, e.g. modified KdV equation (mKdV) [39, 40] and NLS[41], can also be obtained by applying the degenerate DT method to the Ablowitz-Kaup-Newell-Segur (AKNS) hierarchy[42].

Essentially, one of the RWs' characteristics is the height of the fundamental pattern[43–47]. Two sorts of patterns, fundamental patterns and decomposed patterns, are discussed in detail in Refs. [48, 49]. A wide range of decomposed patterns of the nth-order RWs of NLS have been constructed[34, 50], such as triangular pattern[51], circular pattern[52] with one $(2(n-1)+1)$-peak ring outside and $(n-2)$th-order RW inside, dicyclic pattern with double $(2(n-2)+1)$-peak rings outside and $(n-4)$th-order RW inside, tricyclic pattern with triple $(2(n-3)+1)$-peak rings outside and $(n-6)$th-order RW inside, etc. Besides the peak height and various RW patterns, another essential algebraic characteristic of RWs is the degree of the denominator (numerator) polynomial of the rational solution, which is twice the number of the 1st-order RW peaks in the completely decomposed pattern[48]. For example, Table 1 in Refs. [41, 43] shows that the nth-order RWs of NLS possess $n(n+1)$ degrees of $F(x,t)$, which means that the completely decomposed patterns of RWs have $n(n+1)/2$ 1st-order RW peaks.

However, in a variety of physical contexts, several waves rather than a single one need to be considered, since numerous physical phenomena require modeling waves with two or more components in order to account for different modes, frequencies, or polarizations. One important example is the well-known Manakov system[53] in optical systems in regard to the resonance phenomena. In these circumstances, RWs should be described by the solutions of multi-component systems of equations rather than by the single-component models. Under certain conditions, the dispersion relation allows for resonances, and multiple-scale perturbation method shows that the amplitudes of two or more monochromatic waves couple to each other leading to nonlinear partial differential equation (PDE) systems, even an integrable system. The simplest of such integrable systems is the Manakov system (also known as the 2-component NLS (2CNLS), vector NLS and coupled NLS), given by the following two coupled equations[53]:

$$\begin{cases}\mathbf{i}q_{1t}+q_{1xx}+2\left(|q_1|^2+|q_2|^2\right)q_1=0,\\ \mathbf{i}q_{2t}+q_{2xx}+2\left(|q_1|^2+|q_2|^2\right)q_2=0.\end{cases}\tag{2}$$

Here, $q_j=q_j(x,t)$, $(j=1,2)$. The DT method for 2CNLS has been presented in e.g. Ref. [54] and for N-component NLS (NCNLS) in Ref. [55]. Using the n-fold DT, the n-breather solutions of 2CNLS can be derived by the "seed" solution – i.e., a plane wave solution.

Besides the envelope solitons, the NCNLS also admits a class of localized structure which has been significant interest in space-time localized solutions undergoing periodic energy exchange with a finite background. In the recent decade, the degenerate DT method has been used to construct rational solutions[56–58] and semi-rational solutions of 2CNLS[35, 59] as well. The patterns of 3CNLS are also discussed in e.g. Refs.[60, 61], which show that the 2nd-order RWs of 3CNLS possess five-, seven- and even nine-peak patterns as in Figs. 3-5[60]. These solutions of a multi-component system have a remarkable nonvanishing boundary, which leads to the significant difficulties in solving process by IST[62]. For example, only solitons of the defocusing 3CNLS have been solved in Ref. [62] by IST.

In the studies of the RWs for a multi-component system, the first important problem is to find critical condition for this solution. The condition can automatically imply the critical value of λ_0 in order to construct RWs from breathers. We shall solve this problem by proposing a specialized scheme, in which two techniques are used: 1) introducing two nilpotent Lax matrices by gauge transformation and 2) finding a new equivalent fundamental matrix $\boldsymbol{G}$ by series multisections of eigenfunctions. Another important problem is to investigate what are the characteristics of a multi-component system, such as the degree of the polynomials in the high-order rational solutions. In this paper, first a set of classified rational solutions of NCNLS will be constructed, and the degree of them will be investigated and summarized. Some decomposed patterns of RWs of NCNLS will also be illustrated.

This paper is organized as follows. In Section 2, the 2nd-order flow of the multi-component AKNS, (i.e. multi-component NLS equation) is introduced. In Section 3, two theorems about DT are reformulated by augmented matrix. In Section 4, the critical condition to obtain rational solutions is given. In Section 5, the series multisections of vector eigenfunction are taken as fundamental eigenfunction to construct the rational solutions by the degenerate DT. In Section 6, the characteristics of rational solutions of the NCNLS are summarized. In Section 7, the rational solutions of the 3rd-order flow of the multi-component AKNS (i.e. multi-component complex modified KdV equation) are constructed in brief and the characteristics of these solutions are obtained again. In Section 8, the semi-rational solutions of the multi-component AKNS are discussed shortly. In Section 9, the conclusions are presented.

2 | MULTI-COMPONENT AKNS HIERARCHY

N-component AKNS hierarchy[63] results from the compatibility condition $(\boldsymbol{\phi}_x)_t = (\boldsymbol{\phi}_t)_x$ of the following Lax pair:

$$\begin{cases} \boldsymbol{\phi}_x = \boldsymbol{M}\boldsymbol{\phi}, \\ \boldsymbol{\phi}_t = \boldsymbol{N}\boldsymbol{\phi}, \end{cases} \tag{3}$$

where eigenfunction $\boldsymbol{\phi} = \boldsymbol{\phi}(x,t)$ is a column vector of dimension $N+1$, and square matrices $\boldsymbol{M}$ and $\boldsymbol{N}$ are matrix polynomials with respect to the complex iso-spectral parameter λ:

$$\begin{cases} \boldsymbol{M} = \lambda \boldsymbol{U} + \boldsymbol{V}, \\ \boldsymbol{N} = \lambda^m \boldsymbol{V}_m + \cdots + \lambda \boldsymbol{V}_1 + \boldsymbol{V}_0. \end{cases} \tag{4}$$

Here,

$$\boldsymbol{U} = \begin{pmatrix} -\mathbf{i} & \mathbf{0} \\ \mathbf{0} & \mathbf{i}\boldsymbol{I}_N \end{pmatrix}, \boldsymbol{V} = \begin{pmatrix} 0 & \boldsymbol{q} \\ \boldsymbol{r} & \mathbf{0} \end{pmatrix}, \tag{5}$$

$\boldsymbol{I}_N$ denotes the N-by-N identity matrix, $\mathbf{0}$ denotes the zero matrix and m stands for the order of the multi-component AKNS flow. Potential functions $\boldsymbol{q} = (q_1, q_2, \cdots, q_N)$ and $\boldsymbol{r} = (r_1, r_2, \cdots, r_N)^T$ are row and column vectors, respectively. The superscript "T" represents matrix transposition.

According to the compatibility condition, Lax pair (3) yields the zero-curvature equation $\boldsymbol{M}_t - \boldsymbol{N}_x + [\boldsymbol{M}, \boldsymbol{N}] = 0$. The simplest and important nontrivial example, NCNLS, can be derived in term of the zero-curvature equation by the complementary restriction (reduction condition):

$$\boldsymbol{r} = -\boldsymbol{q}^\dagger, \tag{6}$$

at the 2nd-order flow (viz. $m = 2$). Here, $\dagger$ denotes the Hermitian conjugation.
As a result, the temporal part matrix $\boldsymbol{N}$ for the NCNLS reduces to

$$\boldsymbol{N} = 2\lambda^2 \boldsymbol{U} + 2\lambda \boldsymbol{V} + \boldsymbol{U}\left(\boldsymbol{V}^2 - \boldsymbol{V}_x\right). \tag{7}$$

Therefore, the NCNLS reads as

$$\mathbf{i}\boldsymbol{q}_t + \boldsymbol{q}_{xx} + 2\boldsymbol{q}\boldsymbol{q}^\dagger \boldsymbol{q} = 0, \tag{8}$$

that possesses a periodic "seed" solution $\boldsymbol{q}^{[0]}$:

$$\boldsymbol{q}^{[0]} = \boldsymbol{c}\boldsymbol{E}. \tag{9}$$

Here, $\boldsymbol{E} = \exp(\mathbf{diag}(\boldsymbol{\theta}))$, $\boldsymbol{\theta} = \mathbf{i}(\boldsymbol{a}x + \boldsymbol{b}t)$, $\boldsymbol{a} = (a_1, a_2, \cdots, a_N)$, $\boldsymbol{b} = (b_1, b_2, \cdots, b_N)$, $\boldsymbol{c} = (c_1, c_2, \cdots, c_N)$, with $a_j, c_j \in \mathbb{R}$, and b_j satisfying the dispersion relation of NCNLS:

$$b_j = 2c^2 - a_j^2, \quad \left(c^2 = \sum_{j=1}^N c_j^2\right). \tag{10}$$

3 | DARBOUX TRANSFORMATION

In this section, by referring to Ref. [55], the DT of NCNLS will be reformulated by augmented matrix based on the preceding works[38, 56].

Using the gauge transformation $\boldsymbol{T}^{[1]}$:

$$\boldsymbol{T}^{[1]} = \boldsymbol{T}^{[1]}(\lambda) = \lambda \boldsymbol{I}_{N+1} - \boldsymbol{Q}_0, \qquad \boldsymbol{Q}_0 = \begin{pmatrix} A_0(x,t) & \boldsymbol{B}_0(x,t) \\ \boldsymbol{C}_0(x,t) & \boldsymbol{D}_0(x,t) \end{pmatrix}, \tag{11}$$

the seed solution $(\boldsymbol{\phi}^{[0]}; \boldsymbol{q}^{[0]})$ of Lax pair (3) can be transformed to a new solution:

$$\boldsymbol{\phi}^{[1]} = \boldsymbol{T}^{[1]} \boldsymbol{\phi}^{[0]},$$

that satisfies

$$\begin{cases} \boldsymbol{\phi}_x^{[1]} = \boldsymbol{M}^{[1]} \boldsymbol{\phi}^{[1]}, \\ \boldsymbol{\phi}_t^{[1]} = \boldsymbol{N}^{[1]} \boldsymbol{\phi}^{[1]}, \end{cases} \tag{12}$$

and,

$$\begin{cases} \boldsymbol{M}^{[1]} = \lambda \boldsymbol{U} + \boldsymbol{V}^{[1]}, \\ \boldsymbol{N}^{[1]} = 2\lambda^2 \boldsymbol{U} + 2\lambda \boldsymbol{V}^{[1]} + \boldsymbol{U}\left(\boldsymbol{V}^{[1]2} - \boldsymbol{V}_x^{[1]}\right). \end{cases} \tag{13}$$

Here,

$$\boldsymbol{V}^{[1]} = \begin{pmatrix} 0 & \boldsymbol{q}^{[1]} \\ \boldsymbol{r}^{[1]} & \boldsymbol{0} \end{pmatrix}, \tag{14}$$

and the new potential functions retain the reduction condition $\boldsymbol{r}^{[1]} = -\boldsymbol{q}^{[1]\dagger}$, which implies that $\boldsymbol{C}_0 = -\boldsymbol{B}_0^{\dagger}$.

By a tedious calculation, the one-fold DT for NCNLS[55, 56] can now be derived from the coefficients of λ in the following equations:

$$\begin{cases} \boldsymbol{M}^{[1]} \boldsymbol{T}^{[1]} = \boldsymbol{T}_x^{[1]} + \boldsymbol{T}^{[1]} \boldsymbol{M}^{[0]}, \\ \boldsymbol{N}^{[1]} \boldsymbol{T}^{[1]} = \boldsymbol{T}_t^{[1]} + \boldsymbol{T}^{[1]} \boldsymbol{N}^{[0]}. \end{cases} \tag{15}$$

In this paper, to unify the determinant representation form of solutions, hereby, we rewrite the Theorem 2 in Ref. [55] follows.

Theorem 1. Let $(\boldsymbol{\phi}^{[0]}; \boldsymbol{q}^{[0]})$ be a seed solution of the eigenfunction and potential function in Lax pair (3), then the new eigenfunction and potential function $(\boldsymbol{\phi}^{[1]}; \boldsymbol{q}^{[1]})$ generated by the one-fold DT (11) are expressed as

$$\boldsymbol{\phi}^{[1]} = \boldsymbol{T}^{[1]} \boldsymbol{\phi}^{[0]}, \qquad \boldsymbol{q}^{[1]} = \boldsymbol{q}^{[0]} - 2\mathbf{i}\boldsymbol{B}_0, \tag{16}$$

where, $(A_0, \boldsymbol{B}_0)^T$ is the solution of the following system of linear equantions:

$$\begin{pmatrix} f_{11} & f_{12} & f_{13} & \cdots & f_{1,N+1} \\ -f_{12}^* & f_{11}^* & 0 & \cdots & 0 \\ -f_{13}^* & 0 & f_{11}^* & \cdots & 0 \\ \vdots & \vdots & \vdots & \ddots & \vdots \\ -f_{1,N+1}^* & 0 & 0 & \cdots & f_{11}^* \end{pmatrix} \begin{pmatrix} A_0 \\ \\ \boldsymbol{B}_0^T \end{pmatrix} = \begin{pmatrix} \lambda_1 f_{11} \\ -\lambda_1^* f_{12}^* \\ -\lambda_1^* f_{13}^* \\ \vdots \\ -\lambda_1^* f_{1,N+1}^* \end{pmatrix}, \tag{17}$$

of which $(f_{11}, f_{12}, \cdots, f_{1,N+1})^T = \boldsymbol{\phi}^{[0]}\Big|_{\lambda=\lambda_1}$ is an eigenfunction of Lax pair (3) associated with eigenvalue λ_1.

Here, asterisk denotes complex conjugation. According to Theorem 1, the system of linear equantions (17) can be abbreviated as an augmented matrix $\boldsymbol{\Delta}^{[1]} = \left(\Delta^{[1,0]} \mid \boldsymbol{\beta}^{[1,1]}\right)$ in the absence of ambiguity, where $\Delta^{[j,\ell]} = \Delta^{[j,\ell]}(\boldsymbol{f}_j, \lambda_j; \ell)$ is defined by

$$\Delta^{[j,\ell]} \triangleq \begin{pmatrix} \lambda_j^\ell f_{j1} & \lambda_j^\ell f_{j2} & \lambda_j^\ell f_{j3} & \cdots & \lambda_j^\ell f_{j,N+1} \\ -(\lambda_j^\ell f_{j2})^* & (\lambda_j^\ell f_{j1})^* & 0 & \cdots & 0 \\ -(\lambda_j^\ell f_{j3})^* & 0 & (\lambda_j^\ell f_{j1})^* & \cdots & 0 \\ \vdots & \vdots & \vdots & \ddots & \vdots \\ -(\lambda_j^\ell f_{j,N+1})^* & 0 & 0 & \cdots & (\lambda_j^\ell f_{j1})^* \end{pmatrix}, \tag{18}$$

and vector $\boldsymbol{\beta}^{[j,\ell]}$ is the first column of $\Delta^{[j,\ell]}$. Here, $\boldsymbol{f}_j = (f_{j1}, f_{j2}, \cdots, f_{j,N+1})^T \triangleq \boldsymbol{\phi}^{[0]}\Big|_{\lambda=\lambda_j}$ is an eigenfunction of Lax pair (3) associated with eigenvalue λ_j.

Iteration of DT and ansatz of $\boldsymbol{T}^{[n]}$:

$$\boldsymbol{T}^{[n]} = \boldsymbol{T}^{[n]}(\lambda) = \lambda^n \boldsymbol{I}_{N+1} - \sum_{j=0}^{n-1} \lambda^j \boldsymbol{Q}_j, \quad \boldsymbol{Q}_j = \begin{pmatrix} A_j(x,t) & \boldsymbol{B}_j(x,t) \\ \boldsymbol{C}_j(x,t) & \boldsymbol{D}_j(x,t) \end{pmatrix}, \tag{19}$$

with $\boldsymbol{C}_j = -\boldsymbol{B}_j^{\dagger}$, the n-fold DT for NCNLS can be derived by a similar way as in e.g. Refs. [55, 56]. For convenience, we rewrite the determinant representation of the theorem in the following form.

Theorem 2. Let $(\boldsymbol{\phi}^{[0]}; \boldsymbol{q}^{[0]})$ be a solution of the eigenfunction and potential function in Lax pair (3), then the new eigenfunction and potential function $(\boldsymbol{\phi}^{[n]}; \boldsymbol{q}^{[n]})$ generated by the n-fold DT (19) are expressed as

$$\boldsymbol{\phi}^{[n]} = \boldsymbol{T}^{[n]}\boldsymbol{\phi}^{[0]}, \qquad \boldsymbol{q}^{[n]} = \boldsymbol{q}^{[0]} - 2\mathbf{i}\boldsymbol{B}_{n-1}, \tag{20}$$

where, $(A_0, \boldsymbol{B}_0, A_1, \boldsymbol{B}_1, \cdots, A_{n-1}, \boldsymbol{B}_{n-1})^T$ is the solution of the system of linear equations contained in the following augmented matrix $\boldsymbol{\Delta}^{[n]}$:

$$\boldsymbol{\Delta}^{[n]} = \left(\begin{array}{cccc|c} \Delta^{[1,0]} & \Delta^{[1,1]} & \cdots & \Delta^{[1,n-1]} & \boldsymbol{\beta}^{[1,n]} \\ \Delta^{[2,0]} & \Delta^{[2,1]} & \cdots & \Delta^{[2,n-1]} & \boldsymbol{\beta}^{[2,n]} \\ \vdots & \vdots & \ddots & \vdots & \vdots \\ \Delta^{[n,0]} & \Delta^{[n,1]} & \cdots & \Delta^{[n,n-1]} & \boldsymbol{\beta}^{[n,n]} \end{array}\right), \tag{21}$$

of which $\Delta^{[j,k]}$ $(k = 0, 1, \cdots, n-1)$ and $\boldsymbol{\beta}^{[j,n]}$ are defined by Eq. (18) associated with n distinct eigenvalues λ_j $(j = 1, 2, \cdots, n)$.

According to the theorem above, vector eigenfunction $\boldsymbol{\phi}^{[0]}$ is regarded as a generation function of high-order solution. The n-soliton and n-breather solutions of NCNLS can be obtained by n-fold DT given by Eq. (20) with n distinct eigenvalues λ_j $(j = 1, 2, \cdots, n)$, i.e., using non-degenerate n-fold DT. Next, we will now discuss a specific degenerate case of n-fold DT, by setting all λ_j approach to a particular value λ_0, such that an nth-order breather solution will be converted into an nth-order rational solution. A key point in this process is to find critical condition to implement this interesting conversion.

4 | CRITICAL CONDITION FOR RATIONAL SOLUTIONS OF NCNLS

In this section, using two complex parameters m_0 and n_0 introduced in a gauge transformation, a pair of nilpotent matrices and an eigenfunction with polynomial entries will be derived to construct the rational solutions of NCNLS. The construction details of the nilpotent matrices are shown as follows.

As the "seed" solution $\boldsymbol{q}^{[0]}$ (9) is a plane wave solution, using the gauge transformation $\boldsymbol{\varphi} = \boldsymbol{T}_0\boldsymbol{\phi}$, the Lax pair (3) can be converted to the homogeneous linear differential equations,

$$\begin{cases} \boldsymbol{\varphi}_x = \boldsymbol{M}_0\boldsymbol{\varphi}, \\ \boldsymbol{\varphi}_t = \boldsymbol{N}_0\boldsymbol{\varphi}, \end{cases} \tag{22}$$

where,

$$\boldsymbol{T}_0 = \mathbf{diag}\,(1, \boldsymbol{E}) \cdot \exp\left(\mathbf{i}\left(m_0 x + n_0 t\right)\right), \tag{23}$$

m_0 and n_0 are two complex constants, and

$$\boldsymbol{M}_0 = \mathbf{i}\Big(\mathbf{diag}\,(-2\lambda, \boldsymbol{a}) + (\lambda + m_0)\boldsymbol{I}_{N+1}\Big) + \begin{pmatrix} 0 & \boldsymbol{c} \\ -\boldsymbol{c}^T & \boldsymbol{0} \end{pmatrix}, \tag{24}$$

$$\boldsymbol{N}_0 = \mathbf{i}\widetilde{\boldsymbol{M}}_0^2 + 2\lambda\widetilde{\boldsymbol{M}}_0 + \mathbf{i}(\lambda^2 + 2c^2 + n_0)\boldsymbol{I}_{N+1}, \qquad (\widetilde{\boldsymbol{M}}_0 \triangleq \boldsymbol{M}_0 - \mathbf{i}m_0\boldsymbol{I}_{N+1}). \tag{25}$$

Apparently, the characteristic polynomial $P(\kappa)$ of $\boldsymbol{M}_0$,

$$P(\kappa) = \left|\kappa\boldsymbol{I}_{N+1} - \boldsymbol{M}_0\right| = \kappa^{N+1} + \sum_{j=0}^{N} \mathbf{i}^{N-j+1}\sigma_j\kappa^j, \tag{26}$$

has $N+1$ eigenvalues $\kappa_j \in \mathbb{C}, (j = 1, 2, \cdots, N+1)$. Because of Eq. (25), each eigenvalue ω_j of $\boldsymbol{N}_0$ corresponding to κ_j satisfies

$$\omega_j = \mathbf{i}\widetilde{\kappa}_j^2 + 2\lambda\widetilde{\kappa}_j + \mathbf{i}(\lambda^2 + 2c^2 + n_0), \quad (\widetilde{\kappa}_j \triangleq \kappa_j - \mathbf{i}m_0). \tag{27}$$

Since matrices $\boldsymbol{M}_0$ and $\boldsymbol{N}_0$ commute and share the same eigenvector $\boldsymbol{\eta}_j, (j = 1, 2, \cdots, N+1)$, the fundamental matrix $\boldsymbol{\Psi}_0$ of system (22) can be achieved in a non-degenerate case,

$$\boldsymbol{\Psi}_0(x, t) = \exp\left(\boldsymbol{M}_0 x + \boldsymbol{N}_0 t\right) = \boldsymbol{\Phi}\boldsymbol{\Lambda}\boldsymbol{\Phi}^{-1}, \tag{28}$$

where the diagonal matrix $\boldsymbol{\Lambda} = \exp\left(\mathbf{diag}\,(\boldsymbol{\kappa}x + \boldsymbol{\omega}t)\right)$, $\boldsymbol{\kappa} = (\kappa_1, \kappa_2 \cdots, \kappa_{N+1})$, $\boldsymbol{\omega} = (\omega_1, \omega_2 \cdots, \omega_{N+1})$ and $\boldsymbol{\Phi} = (\boldsymbol{\eta}_1, \boldsymbol{\eta}_2, \cdots, \boldsymbol{\eta}_{N+1})$. Therefore, the vector eigenfunction of system (22) can be written as

$$\boldsymbol{\varphi} = \boldsymbol{\Psi}_0\zeta_0 = \boldsymbol{\Phi}\boldsymbol{\Lambda}\boldsymbol{\zeta}, \tag{29}$$

where, $\boldsymbol{\zeta} \triangleq \boldsymbol{\Phi}^{-1}\zeta_0$ is an arbitrary non-zero constant vector due to the arbitrariness of the constant vector ζ_0.

In this paper, we mainly focus on the asymptotic behavior of complete resonant interaction, that is the case of eigenvalue of multiplicity $N+1$ of $\boldsymbol{M}_0$. One of the parameters introduced in Eq. (23), m_0, will be used to translate the eigenvalue κ of multiplicity $N+1$ to the original point, which will lead $\boldsymbol{M}_0$ to be a nilpotent matrix. Another parameter, n_0, will translate the multiple eigenvalue ω of $\boldsymbol{N}_0$ to the original point as well.

Actually, to obtain the zero-eigenvalues of matrices $\boldsymbol{M}_0$ and $\boldsymbol{N}_0$ associated with multiplicity $N+1$, simply and conveniently, let

$$\sigma_j = 0\,(j = 0, 1, 2, \cdots, N) \text{ and } \mathrm{Trace}\,(\boldsymbol{N}_0) = 0, \tag{30}$$

based on Eqs. (26) and (27). Obviously, Eq. (30) provides critical condition to obtain the eigenfunction with polynomial entries for the system (22).

Firstly, the condition $\sigma_N = 0$ (equivalent to $\mathrm{Trace}\,(\boldsymbol{M}_0) = 0$) yields

$$m_0 = \frac{-1}{N+1}\left((N-1)\lambda + \sum_{j=1}^{N} a_j\right), \tag{31}$$

and the condition $\mathrm{Trace}\,(\boldsymbol{N}_0) = 0$ yields

$$n_0 = \frac{-1}{N+1}\left(2(N-1)\lambda^2 + 2Nc^2 - \sum_{j=1}^{N} a_j^2\right). \tag{32}$$

Secondly, by substituting Eq. (31) into the condition $\sigma_{N-1} = 0$, subsequently, it implies that

$$\left(\lambda + \frac{1}{2N}\sum_{j=1}^{N} a_j\right)^2 + \frac{N+1}{4N^2}\left(2Nc^2 + \sum_{1\leqslant i<j\leqslant N}(a_i - a_j)^2\right) = 0. \tag{33}$$

With at least one of $c_j\,(j = 1, 2, \cdots, N)$ being non-zero, Eq. (33) gives rise to a pair of distinct complex (non-real) conjugate roots λ_0 and λ_0^*, namely the critical value of the spectral parameter λ:

$$\lambda_0 = -\frac{1}{2N}\sum_{j=1}^{N} a_j + \mathbf{i}\frac{\sqrt{N+1}}{2N}\sqrt{2Nc^2 + \sum_{1\leqslant i<j\leqslant N}(a_i - a_j)^2}. \tag{34}$$

Note that, setting $\lambda_j = \lambda_0 + \epsilon^{N+1}$ in the n-fold DT given by Eq. (20) under the critical condition (30), $q^{[n]}$ becomes an indeterminate form $\frac{0}{0}$ that results in an nth-order rational solutions of the NCNLS by the limit $\epsilon \to 0$, according to L'Hospital's rule. Therefore Eq. (30) is also a critical condition to achieve rational solutions of the NCNLS. Due to the extremely tedious formula of the breather solutions given by Eq. (20), it is a challenge to find a simple expression of the critical value of λ_0 in order to construct rational solutions from breathers, as we have carried it out for the single component NLS[34, 36].

Thirdly, it can be proven that all of the coefficients $\sigma_j, (j = 0, 1, \cdots, N)$ in Eq. (26) are polynomials over $\mathbb{Z}$ with respect to a_j, c_j, m_0, and λ. As for the rest conditions $\sigma_j = 0, (j = 0, 1, \cdots, N-2)$, if $N \geqslant 2$, σ_j can be reduced to linear equations $\widetilde{\sigma}_j = 0$ in λ by Eqs. (31) and (33). Because of the $2N$ parameters a_j and $c_j (j = 1, 2, \cdots, N)$ in $\widetilde{\sigma}_j$ are real, except λ, the two coefficients of $\widetilde{\sigma}_j$ in λ should be vanishing. Based on the brief analysis above, there are two free real variables available among these $2N$ parameters. Without loss of generality, we use two-dimensional coordinate space (a_1, c_1), in this context, to present the critical condition explicitly.

Finally, substituting the values of parameters $(a_j, c_j, 2 \leqslant j \leqslant N)$ back into Eq. (34) leads to an explicit formula of λ_0, further substituting them back into Eqs. (31) and (32) associated with $\lambda = \lambda_0$, we get two explicit formulas for m_0 and n_0. We may now claim that constants m_0 and n_0 are independent of λ under the critical condition given by Eq. (30), which is an important observation for us in order to construct degenerate DT in next section.

From the above, the nilpotent matrices associated with the fundamental matrix can be obtained by Eq. (30). For instance, in the case of $N = 2$, Eq. (30) yields

$$\lambda_0 = \frac{1}{4}\left(-1 + 3\sqrt{3}\mathbf{i}\right)c_1 - \frac{1}{2}a_1, \tag{35}$$

and

$$\begin{cases} c_2 &= c_1, \\ a_2 &= a_1 + c_1, \\ m_0 &= \frac{1}{4}\left(-1 - \sqrt{3}\mathbf{i}\right)c_1 - \frac{1}{2}a_1, \\ n_0 &= \frac{1}{4}\left(-5 + \sqrt{3}\mathbf{i}\right)c_1^2 + \frac{1}{2}\left(1 + \sqrt{3}\mathbf{i}\right)a_1c_1 + \frac{1}{2}a_1^2. \end{cases} \tag{36}$$

Thus, $\boldsymbol{M}_0$ degenerates to a nilpotent matrix,

$$\boldsymbol{M}_0 = \begin{pmatrix} \sqrt{3} & 1 & 1 \\ -1 & \mathbf{i}\varepsilon_1 & 0 \\ -1 & 0 & -\mathbf{i}\varepsilon_2 \end{pmatrix} c_1 = \boldsymbol{Q}\boldsymbol{J}_3\boldsymbol{Q}^{-1},$$

where,

$$\boldsymbol{Q} = \begin{pmatrix} c_1^2 & \sqrt{3}c_1 & 1 \\ -\mathbf{i}\epsilon_2 c_1^2 & -c_1 & 0 \\ \mathbf{i}\epsilon_1 c_1^2 & -c_1 & 0 \end{pmatrix}, \boldsymbol{J}_3 = \begin{pmatrix} 0 & 1 & 0 \\ 0 & 0 & 1 \\ 0 & 0 & 0 \end{pmatrix},$$

and the unit root ε_j is defined as

$$\varepsilon_j = \exp\left(\frac{2j\pi\mathbf{i}}{N+1}\right), (j = 0, 1, \cdots, N). \tag{37}$$

Therefore, as a consequence of Eq. (25), the temporal part matrix $\boldsymbol{N}_0$ can be reduced to a nilpotent matrix by $\boldsymbol{Q}$ as well. Thereby, Eq. (28) will be similar to an upper triangular matrix with polynomial entries:

$$\boldsymbol{J} = \boldsymbol{Q}^{-1}\exp\left(\boldsymbol{M}_0 x + \boldsymbol{N}_0 t\right)\boldsymbol{Q} = \begin{pmatrix} 1 & \chi & \frac{1}{2}\chi^2 + \mathbf{i}t \\ 0 & 1 & \chi \\ 0 & 0 & 1 \end{pmatrix}, \tag{38}$$

where, $\chi = x - (2a_1 + c_1 - \sqrt{3}\mathbf{i}c_1)t$. Then, the vector eigenfunction (29) with polynomial entries can be obtained:

$$\boldsymbol{\varphi} = \boldsymbol{Q}\boldsymbol{J}\boldsymbol{\zeta} = \begin{pmatrix} c_1^2 & (c_1\chi + \sqrt{3})c_1 & \left(\frac{1}{2}\chi^2 + \mathbf{i}t\right)c_1^2 + \sqrt{3}c_1\chi + 1 \\ -\mathbf{i}\epsilon_2\, c_1^2 & -(\mathbf{i}\epsilon_2 c_1\chi + 1)c_1 & -(\mathbf{i}\epsilon_2 c_1\left(\frac{1}{2}\chi^2 + \mathbf{i}t\right) + \chi)c_1 \\ \mathbf{i}\epsilon_1\, c_1^2 & (\mathbf{i}\epsilon_1 c_1\chi - 1)c_1 & (\mathbf{i}\epsilon_1 c_1\left(\frac{1}{2}\chi^2 + \mathbf{i}t\right) - \chi)c_1 \end{pmatrix}\boldsymbol{\zeta}. \tag{39}$$

In the following, let $\lambda_j \to \lambda_0$ under the critical condition given by Eq. (30), the non-degenerate eigenfunction (29) will tend to be a vector with polynomial entries without an exponent factor. Using the perturbation method and degenerate DT by setting $\lambda_j = \lambda_0 + \epsilon^{N+1}$ and higher-order Taylor expansion of eigenfunction of Eq. (20), the rational solutions of NCNLS will be constructed in the next sections.

5 | NEW RATIONAL SOLUTIONS OF NCNLS

In this section, a set of series multisections, derived from the vector eigenfunction containing exponent factor in a non-degenerate case, are used as the fundamental generation functions to construct a family of rational solutions.

First of all, we present a specific form of the vector eigenfunction. Setting the constant vector as $\boldsymbol{\zeta} = \exp\left(\mathbf{diag}\left(\boldsymbol{s}^0\right)\right)\boldsymbol{\gamma}$, or,

$$\zeta_j = \gamma_j \exp(s_j^0) = \gamma_j \exp(\kappa_j x_j^0 + \omega_j t_j^0), (j = 1, 2, \cdots, N+1),$$

thus, the constants x_j^0 and t_j^0 are translational displacements along the $x-$ and $t-$ axes, respectively. In this paper, without loss of generality, we simply concentrate on the offset x_j^0, that is to say, let $t_j^0 = 0$ or $s_j^0 = \kappa_j x_j^0$ only. So, $\boldsymbol{\varphi}$ can be rewritten as

$$\boldsymbol{\varphi} = \boldsymbol{\Phi}\boldsymbol{\Lambda}\exp\left(\mathbf{diag}\left(\boldsymbol{s}^0\right)\right)\boldsymbol{\gamma} = (\boldsymbol{\psi}_1, \boldsymbol{\psi}_2, \cdots, \boldsymbol{\psi}_{N+1})\boldsymbol{\gamma} \triangleq \boldsymbol{\Psi}\boldsymbol{\gamma}, \tag{40}$$

where, matrix $\boldsymbol{\Psi}$ is an equivalent fundamental matrix of which

$$\boldsymbol{\psi}_j(x, t) = \exp(\kappa_j(x + x_j^0) + \omega_j t)\boldsymbol{\eta}_j,$$

and $\boldsymbol{\gamma}$ is a set of combination coefficients of $\boldsymbol{\psi}_j (j = 1, 2, \cdots, N+1)$.

To obtain the 1st-order rational solutions, the equivalent limit form of $\boldsymbol{\Delta}^{[1]}$, based on the Cramer's rule and L'Hôpital's rule, is required. Let $\lambda_1 = \lambda_0 + \epsilon^{N+1}$ under the critical condition given by Eq. (30). Since $\boldsymbol{\phi} = \boldsymbol{T}_0^{-1}\boldsymbol{\varphi}$ is associated with λ_1 in Eq. (17), the Taylor expansion of each column vector in the fundamental matrix (40), $\boldsymbol{\psi}_j(x, t; \lambda_1)$, is firstly considered:

$$\boldsymbol{\psi}_j(x, t; \lambda_0 + \epsilon^{N+1}) = \sum_{\ell=0}^{\infty} \boldsymbol{u}_{j\ell}\epsilon^{\ell}, \quad \left(\boldsymbol{u}_{j\ell} \triangleq \frac{1}{\ell!}\frac{\partial}{\partial\epsilon^{\ell}}\boldsymbol{\psi}_j\bigg|_{\epsilon=0}\right). \tag{41}$$

Hence, the series multisection of the power series in the above

$$\boldsymbol{\psi}_{jk} = \sum_{\ell=0}^{\infty} \boldsymbol{u}_{j,\ell(N+1)+k} \epsilon^{\ell(N+1)+k}, (k = 0, 1, \cdots, N), \tag{42}$$

has a closed-form expression[64] (see pages from 131-141 for details):

$$\boldsymbol{\psi}_{jk} = \frac{1}{N+1} \sum_{\ell=0}^{N} \varepsilon_1^{-k\ell} \boldsymbol{\psi}_j(x, t; \lambda_0 + (\varepsilon_1^{\ell} \epsilon)^{N+1}), \tag{43}$$

where ε_1 is the primitive $(N+1)$th root of unity, defined by Eq. (37).

Omitting the common factor $1/(N+1)$ in Eq. (43), there exists a set of power series $\boldsymbol{g}_k$ $(k = 0, 1, \cdots, N)$ composed of equally spaced terms, which can be combinated linearly from the original Taylor series of $\boldsymbol{\psi}_j(x, t; \lambda_0 + \epsilon^{N+1})$:

$$\boldsymbol{g}_k = \boldsymbol{\Psi} \boldsymbol{\gamma}_k, \qquad \boldsymbol{\gamma}_k \triangleq (1, \varepsilon_1^{-k}, \varepsilon_1^{-2k}, \cdots, \varepsilon_1^{-Nk})^T. \tag{44}$$

Formally, the series multisection $\boldsymbol{g}_k$ $(k = 0, 1, \cdots, N)$ can be expressed by the power series composed of equally spaced terms:

$$\boldsymbol{g}_k = \sum_{\ell=0}^{\infty} \boldsymbol{v}_{\ell(N+1)+k} \epsilon^{\ell(N+1)+k}. \tag{45}$$

Here, the vector coefficient $\boldsymbol{v}_j = \left(v_{j1}, v_{j2}, \cdots, v_{j,N+1}\right)^T$, on the basis of the exponential threshold k, can be evaluated from Eq. (44).

Thus, matrix $\boldsymbol{G}$,

$$\boldsymbol{G} = (\boldsymbol{g}_0, \boldsymbol{g}_1, \cdots, \boldsymbol{g}_N) = \boldsymbol{\Psi\Gamma}, \qquad \boldsymbol{\Gamma} \triangleq (\boldsymbol{\gamma}_0, \boldsymbol{\gamma}_1, \cdots, \boldsymbol{\gamma}_N), \tag{46}$$

is an equivalent fundamental matrix, since $\boldsymbol{g}_k$ $(k = 0, 1, \cdots, N)$ are linearly independent. In this paper, $\{\boldsymbol{g}_k | k = 0, 1, \cdots, N\}$ are regarded as a family of fundamental eigenfunctions to generate the rational solutions by the degenerate DT. For instance, in the case of $N = 2$, a new fundamental matrix $\boldsymbol{G} = \left(\boldsymbol{g}_0, \boldsymbol{g}_1, \boldsymbol{g}_2\right)$ can be acquired by 3 specific constant vectors $\boldsymbol{\gamma}_0, \boldsymbol{\gamma}_1, \boldsymbol{\gamma}_2$:

$$\boldsymbol{G} = \boldsymbol{\Psi} \begin{pmatrix} 1 & 1 & 1 \\ 1 & \varepsilon_1 & \varepsilon_2 \\ 1 & \varepsilon_2 & \varepsilon_1 \end{pmatrix}, \text{ or, } \begin{cases} \boldsymbol{g}_0 = \boldsymbol{\psi}_{10} + \boldsymbol{\psi}_{20} + \boldsymbol{\psi}_{30}, \\ \boldsymbol{g}_1 = \boldsymbol{\psi}_{11} + \varepsilon_1 \boldsymbol{\psi}_{21} + \varepsilon_2 \boldsymbol{\psi}_{31}, \\ \boldsymbol{g}_2 = \boldsymbol{\psi}_{12} + \varepsilon_2 \boldsymbol{\psi}_{22} + \varepsilon_1 \boldsymbol{\psi}_{32}. \end{cases} \tag{47}$$

Applying the Cramer's rule to get the determinant form of DT as the simplest case, a series of elementary row operations [46] can be performed on the augmented matrix $\boldsymbol{\Delta}^{[1]}$. Then, the one-fold degenerate DT, namely using the simplified matrix $\boldsymbol{B}_0'$ instead of $\boldsymbol{B}_0$, yields the 1st-order RW solution as below.

Theorem 3. Let $\boldsymbol{q}^{[1]}$ be a solution to Eq. (16) with the seed solution given by Eq. (9) and $\lambda_1 = \lambda_0 + \epsilon^{N+1}$ under the critical condition defined by Eq. (30), then the 1st-order RW solution $\boldsymbol{q}_{\mathrm{rw}}^{[1]}$ generated by the one-fold degenerate DT is expressed as

$$\boldsymbol{q}_{\mathrm{rw}}^{[1]} = \left(\boldsymbol{c} - 2\mathbf{i}\boldsymbol{B}_0'\right) \boldsymbol{E}, \tag{48}$$

where, $(A_0', \boldsymbol{B}_0')^T$ is the solution of the system of linear equations contained in the following augmented matrix $\boldsymbol{\Delta}_{\mathrm{rw}}^{[1]}$:

$$\boldsymbol{\Delta}_{\mathrm{rw}}^{[1]} = \left(\begin{array}{ccccc|c} v_{k1} & v_{k2} & v_{k3} & \cdots & v_{k,N+1} & \lambda_0 v_{k1} \\ -v_{k2}^* & v_{k1}^* & 0 & \cdots & 0 & -\lambda_0^* v_{k2}^* \\ -v_{k3}^* & 0 & v_{k1}^* & \cdots & 0 & -\lambda_0^* v_{k3}^* \\ \vdots & \vdots & \vdots & \ddots & \vdots & \vdots \\ -v_{k,N+1}^* & 0 & 0 & \cdots & v_{k1}^* & -\lambda_0^* v_{k,N+1}^* \end{array}\right), \tag{49}$$

of which $(v_{k1}, v_{k2}, v_{k3}, \cdots, v_{k,N+1})^T = \boldsymbol{v}_k, (k = 1, 2, \cdots, N)$ is defined by Eq. (45).

In general, the augmented matrix $\boldsymbol{\Delta}_{\mathrm{rw}}^{[1]}$ can be rewritten as $\boldsymbol{\Delta}_{\mathrm{rw}}^{[1]} = (\Delta_{\mathrm{rw}}^{[1,0]} \mid \boldsymbol{\beta}_{\mathrm{rw}}^{[1,1]})$, where $\boldsymbol{\Delta}_{\mathrm{rw}}^{[j,\ell]} = \Delta_{\mathrm{rw}}^{[j,\ell]}(\boldsymbol{g}_k)$ is defined by

$$\Delta_{\mathrm{rw}}^{[j,\ell]} \triangleq \left(\frac{1}{n_j!} \frac{d^{n_j}}{d\epsilon^{n_j}} \Delta^{[j,\ell]}(\boldsymbol{g}_k, \lambda_0 + \epsilon^{N+1}; \ell)\right)\Bigg|_{\epsilon=0}, \tag{50}$$

$n_j = (j-1)(N+1) + k$, and vector $\boldsymbol{\beta}_{\mathrm{rw}}^{[j,\ell]}$ is the first column of $\Delta_{\mathrm{rw}}^{[j,\ell]}$. Here, $\boldsymbol{g}_k = (g_{k1}, g_{k2}, \cdots, g_{k,N+1})^T$ is defined by Eq. (45).

It should note that the one-fold DT solution is still a plane wave solution in the case of $k = 0$. In addition, using the phase parameters $x_j^0\,(j = 1, 2, \cdots, N+1)$ of the constant vector $\boldsymbol{\zeta}$, the 1st-order RW solution $\boldsymbol{q}_{\mathrm{rw}}^{[1]}$ reads as

$$\boldsymbol{q}_{\mathrm{rw}}^{[1]} = \boldsymbol{q}_{\mathrm{rw}}^{[1]}(x, t; a_1, c_1; x_1^0, x_2^0, \cdots, x_{N+1}^0), \tag{51}$$

which can repsent a variety of the collision models corresponding to the different patterns of the 1st-order RWs. In general, free parameters x_j^0 are mutually independent. For example, let $x_1^0 = -\varepsilon_2 x_2^0 - \varepsilon_1 x_3^0$, and $x_2^0 = 0$ in a 2CNLS system. Then, set phase parameter x_3^0 as $20, \frac{25}{3}, 0, -15$ in sequence, then the twin peaks patterns are shown in Fig. 1, which are analogue and very close to the Figs. 1-3 in Refs. [57, 58].

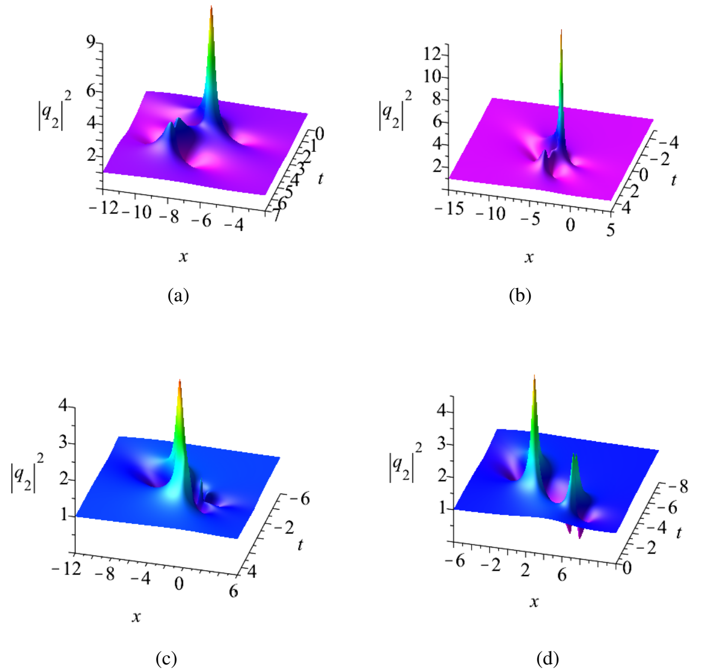

FIGURE 1 The $|q_2|^2$ profiles of the rational solutions of 2CNLS.

In particular, when $x_1^0 = x_2^0 = \cdots = x_{N+1}^0 \triangleq x_0$, as a result, x_0 denotes the translation of RWs on the x-axis. Hereby, the subscript j of x_j^0 can be omitted. Thus, the 1st-order RWs, $\boldsymbol{q}_{\mathrm{rw}}^{[1]}$, can be rewritten as

$$\boldsymbol{q}_{\mathrm{rw}}^{[1]} = \boldsymbol{q}_{\mathrm{rw}}^{[1]}(x, t; a_1, c_1; x_0). \tag{52}$$

In the case of $N = 2$, the fundamental patterns of the 1st-order RWs can be achieved and the profiles of RWs are shown in Fig. 2. Since x_0 is a translation parameter, all the figures in Fig. 2 are fundamental patterns generated by the fundamental eigenfunctions $\boldsymbol{g}_k$ with $k = 1$ and $k = 2$. The profiles in the case of $k = 1$ have only one peak, while two peaks in the case of $k = 2$. It is important to note that Fig. 2(d) is the same as Fig. 1(c), since they are the same figures but with a different angle of view.

To obtain higher order RW solutions, the simplifed form of the augmented matrix $\boldsymbol{\Delta}^{[n]}$ needs constructed. Let $\lambda_j = \lambda_0 + \epsilon^{N+1}\,(j = 1, 2, \cdots, n)$ in sequence, using the Taylor coefficients of power series (45), a simplified augmented matrix $\boldsymbol{\Delta}_{\mathrm{rw}}^{[n]}$ for the nth-order RW solutions can be constructed as

$$\boldsymbol{\Delta}_{\mathrm{rw}}^{[n]} = \boldsymbol{\Delta}_{\mathrm{rw}}^{[n]}(\boldsymbol{g}_k) \triangleq \left(\begin{array}{cccc|c} \Delta_{\mathrm{rw}}^{[1,0]} & \Delta_{\mathrm{rw}}^{[1,1]} & \cdots & \Delta_{\mathrm{rw}}^{[1,n-1]} & \boldsymbol{\beta}_{\mathrm{rw}}^{[1,n]} \\ \Delta_{\mathrm{rw}}^{[2,0]} & \Delta_{\mathrm{rw}}^{[2,1]} & \cdots & \Delta_{\mathrm{rw}}^{[2,n-1]} & \boldsymbol{\beta}_{\mathrm{rw}}^{[2,n]} \\ \vdots & \vdots & \ddots & \vdots & \vdots \\ \Delta_{\mathrm{rw}}^{[n,0]} & \Delta_{\mathrm{rw}}^{[n,1]} & \cdots & \Delta_{\mathrm{rw}}^{[n,n-1]} & \boldsymbol{\beta}_{\mathrm{rw}}^{[n,n]} \end{array}\right). \tag{53}$$

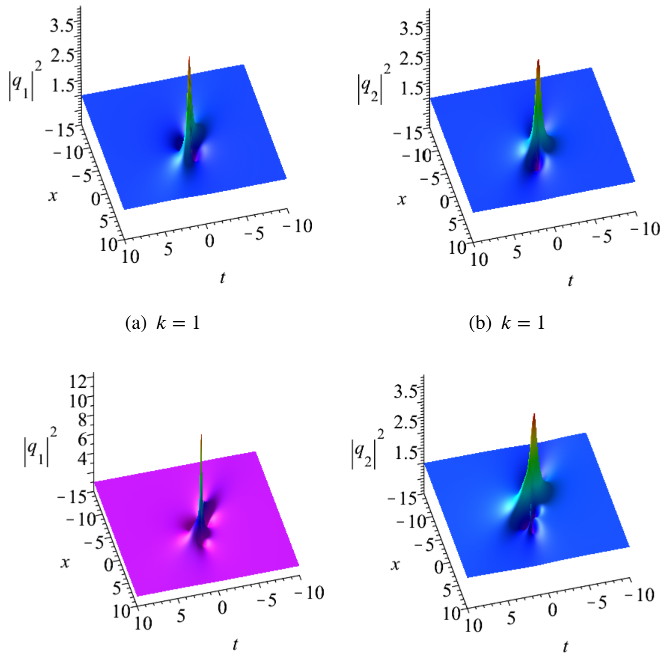

(a) $k = 1$ (b) $k = 1$

(c) $k = 2$ (d) $k = 2$

FIGURE 2 The fundamental pattern of 1st-order RWs of 2CNLS.

The higher-order Taylor expansion comes from the indeterminate form $\frac{0}{0}$ in Eq. (20) due to the limit of $\lambda_j = \lambda_0 + \epsilon^{N+1}$ (i.e., the degenerate DT). Then, n-fold degenerate DT yields nth-order RW solutions as below.

Theorem 4. Let $\boldsymbol{q}^{[n]}$ be a solution to Eq. (20) with the seed solution given by Eq. (9) and $\lambda_j = \lambda_0 + \epsilon^{N+1}\,(j = 1, 2, \cdots, n)$ under the critical condition defined by Eq. (30), then the nth-order RW solution $\boldsymbol{q}_{\mathrm{rw}}^{[n]}$ generated by the n-fold degenerate DT is expressed as

$$\boldsymbol{q}_{\mathrm{rw}}^{[n]} = \left(\boldsymbol{c} - 2\mathbf{i}\boldsymbol{B}'_{n-1}\right)\boldsymbol{E}, \tag{54}$$

where, $(A'_0, \boldsymbol{B}'_0, \cdots, A'_{n-1}, \boldsymbol{B}'_{n-1})^T$ is the solution of the system of linear equations contained in the augmented matrix $\boldsymbol{\Delta}_{\mathrm{rw}}^{[n]}$ defined by Eq. (53).

According to Theorem 4, for the high-order RWs, namely $n \geqslant 2$, each element in the jth $(N+1)$-rows-block of $\boldsymbol{\Delta}_{\mathrm{rw}}^{[n]}$ is the $((j-1)(N+1)+k)$th Taylor coefficient of the corresponding element in the $\boldsymbol{\Delta}^{[n]}$. For instance, the 2nd-order RWs with fundamental pattern of 2CNLS can be achieved by Eq. (53) and the corresponding profiles are shown in Fig. 3 with $k = 1, 2$. Note that the numerator and denominator of B'_1 are shown in **Appendix** A. In addition, the figures with $k = 0$ are omitted due to their similarity on Figs. 2(c) and 2(d), because they only differ by the constant factors ε_1 and ε_2, respectively.

For high-order RW solutions, let $x_0 = s_0 + \sum_{j=1}^{n-1} s_j \epsilon^{j(N+1)}$ in the perturbation expansion of x_0. Thus, the nth-order RWs of NCNLS can be written as

$$\boldsymbol{q}_{\mathrm{rw}}^{[n]} = \boldsymbol{q}_{\mathrm{rw}}^{[n]}(x, t; a_1, c_1; s_0, s_1, \cdots, s_{n-1}), \tag{55}$$

and the phase parameters s_j determine the patterns of RWs. By default, all $s_j = 0\,(j = 0, 1, 2, \cdots, n-1)$, corresponding to the fundamental pattern, are denoted as $x_0 = 0$ or $s_0 = 0$ at this point. In the decomposed patterns, only the non-zero parameters s_j will be listed for convenience.

6 | CHARACTERISTICS OF RWS TO NCNLS

In this section, the degree of polynomial in the denominator of the RW solutions, which is referred briefly as the degree of RWs, will be summed up. The degree is an essential characteristic of RWs, which determines the number of 1st-order RW peaks in a completely decomposed pattern of a high-order RW.

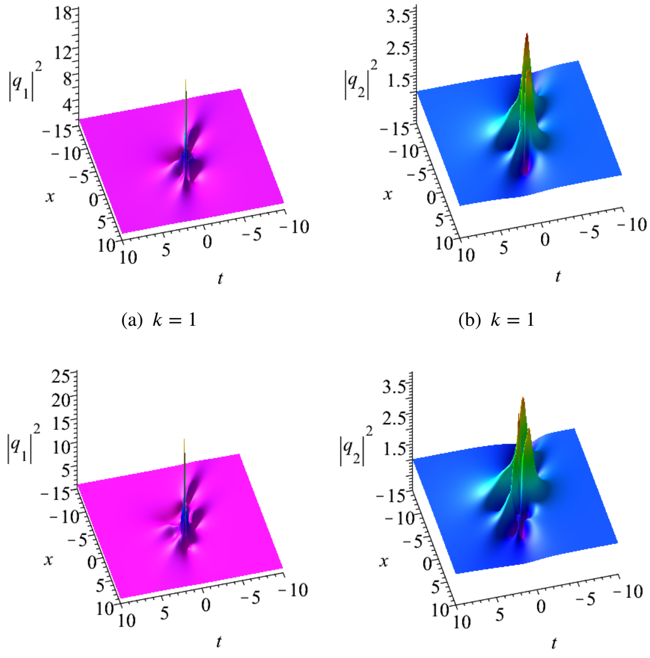

(a) $k = 1$ (b) $k = 1$

(c) $k = 2$ (d) $k = 2$

FIGURE 3 The fundamental pattern of the 2nd-order RWs of 2CNLS.

Conveniently, let us use the function $\deg(k, n, N)$ to denote the degree of the nth-order RW solutions of NCNLS, i.e., the degree of the polynomial in denominator of RW, generated by $\boldsymbol{g}_k$ via the n-fold degenerate DT. Thus, by a lengthy and complicated calculation, it is found that the rational solutions of 2CNLS possess the following results for any parameters s_j, which are confirmed by explicit forms of these solutions up to 5th order.

TABLE 1 $\deg(k, n, N)$ of RWs of 2CNLS

k \ n	1	2	3	4	5
0	0	4	12	24	40
1	2	8	18	32	50
2	4	12	24	40	60

Half value of $\deg(k, n, N)$ determines the maximum number of 1st-order RW peaks in any decomposed RW patterns. In order to illustrate the point with some simple graphs, a couple of parameters values are chosen. For example, let $k = 1, 2$; $n = 2, 3$, and different values of phase parameters s_j to verify the results of $\deg(k, n, 2)$ for 2CNLS in the following three figures.

The decomposed patterns of the 2nd-order RWs of 2CNLS with $a_1 = 0, c_1 = 1, s_1 = 10^3$ are shown in Fig. 4. The figures are all components' profiles generated by the fundamental eigenfunctions $\boldsymbol{g}_k$ with $k = 1, 2$. There is one 4-peak ring outside in both cases of $k = 1$ and 2, while there are 2 peaks inside in the case of $k = 2$ that are similar to Figs. 2(c) and 2(d). Note that there are three peaks for 2nd-order RWs of single component NLS, which are different from the same order RWs for 2CNLS.

The decomposed patterns of the 3rd-order RWs of 2CNLS, generated by fundamental eigenfunction $\boldsymbol{g}_1$ with $a_1 = 0, c_1 = 1$, are shown in Fig. 5. There are 9 peaks in each figure. The figures in the top row have two 4-peak rings outside and a 1-peak inside pattern with $s_1 = 10^3$. The figures in the bottom row have one 7-peak ring outside and another 2-peak inside pattern with $s_2 = 10^5$. The 2 peaks inside are similar to that of Figs. 2(c) and 2(d).

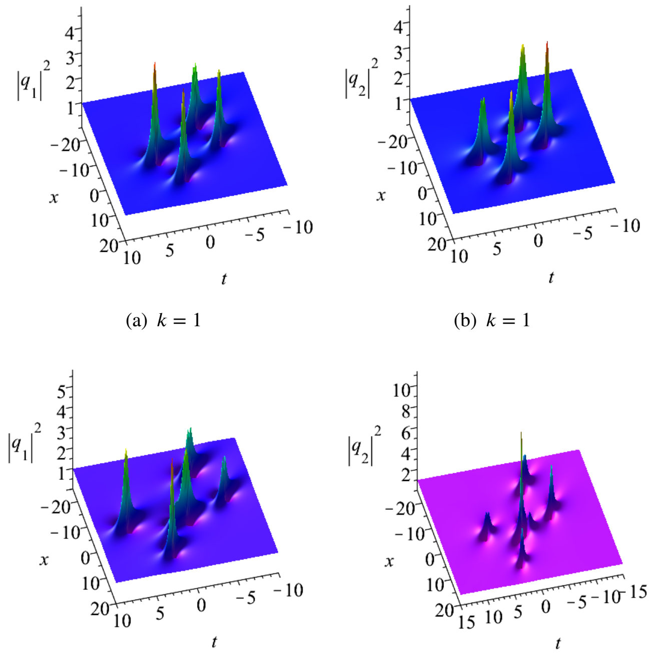

(a) $k = 1$ (b) $k = 1$

(c) $k = 2$ (d) $k = 2$

FIGURE 4 The decomposed patterns of the 2nd-order RWs of 2CNLS.

The circular patterns of the 3rd-order RWs of 2CNLS, generated by fundamental eigenfunction $\boldsymbol{g}_2$ with $a_1 = 0, c_1 = 1$, are shown in Fig. 6. There is a 7-peak circumjacent ring in each figure. The central areas in the top row are fundamental patterns with $s_1 = 0, s_2 = 10^5$, and the bottom row are completely decomposed pattern (7-peak ring outside and 5-peak inside) with $s_1 = 10^4, s_2 = 10^8$.

Figs. 4-6 shown above and other higher-order RW solutions we have calculated indicate the following observation about the distribution of peaks in a decomposed pattern of nth-order RWs: by setting parameter s_{n-1} to be a sufficiently large value and the other parameters s_i to be zeroes, there is a single ring outside consisted by $((N+1)(n-1)+1)$ peaks. Note, by setting parameter s_{n-2} to be a sufficiently large value and the other parameters s_i to be zeroes, there also exist double rings outside, each ring consisting of $((N+1)(n-2)+1)$ peaks in a pattern such as Figs. 5(a) and 5(b).

Case of $N = 3$

To go a step further, in the case of $N = 3$[61], let all the coefficients $\delta_j, (j = 0, 1, 2, 3)$ of the characteristic polynomial (26) and Trace $(\boldsymbol{N}_0)$ be vanishing, consequently, one of the critical conditions of rational solutions could be

$$\begin{cases} a_2 = a_1 - c_1, \\ a_3 = a_1 + c_1, \\ c_2 = c_3 = \sqrt{2}c_1, \end{cases} \text{and,} \begin{cases} \lambda_0 = -\frac{1}{2}a_1 + 2\mathbf{i}c_1, \\ m_0 = -\frac{1}{2}a_1 - \mathbf{i}c_1, \\ n_0 = -\frac{1}{2}a_1(a_1^2 - 18c_1^2) - \mathbf{i}c_1(3a_1^2 - 16c_1^2). \end{cases} \tag{56}$$

Let $\lambda = \lambda_0 + \epsilon^4$, the fundamental matrix $\boldsymbol{G} = \left(\boldsymbol{g}_0, \boldsymbol{g}_1, \boldsymbol{g}_2, \boldsymbol{g}_3\right)$ of (28) can then be obtained

$$\boldsymbol{G} = \boldsymbol{\Psi}\begin{pmatrix} 1 & 1 & 1 & 1 \\ 1 & -\mathbf{i} & -1 & \mathbf{i} \\ 1 & -1 & 1 & -1 \\ 1 & \mathbf{i} & -1 & -\mathbf{i} \end{pmatrix}, \text{or,} \begin{cases} \boldsymbol{g}_0 = \boldsymbol{\psi}_{10} + \boldsymbol{\psi}_{20} + \boldsymbol{\psi}_{30} + \boldsymbol{\psi}_{40}, \\ \boldsymbol{g}_1 = \boldsymbol{\psi}_{11} - \mathbf{i}\boldsymbol{\psi}_{21} - \boldsymbol{\psi}_{31} + \mathbf{i}\boldsymbol{\psi}_{41}, \\ \boldsymbol{g}_2 = \boldsymbol{\psi}_{12} - \boldsymbol{\psi}_{22} + \boldsymbol{\psi}_{32} - \boldsymbol{\psi}_{42}, \\ \boldsymbol{g}_3 = \boldsymbol{\psi}_{13} + \mathbf{i}\boldsymbol{\psi}_{23} - \boldsymbol{\psi}_{33} - \mathbf{i}\boldsymbol{\psi}_{43}. \end{cases} \tag{57}$$

Using the fundamental eigenfunctions $\boldsymbol{g}_k$ in Eq. (57) to generate the augmented matrix $\boldsymbol{\Delta}_{\mathrm{rw}}^{[n]}$ in Eq. (53), it exports the following result in the case of $N = 3$ up to 5th order.

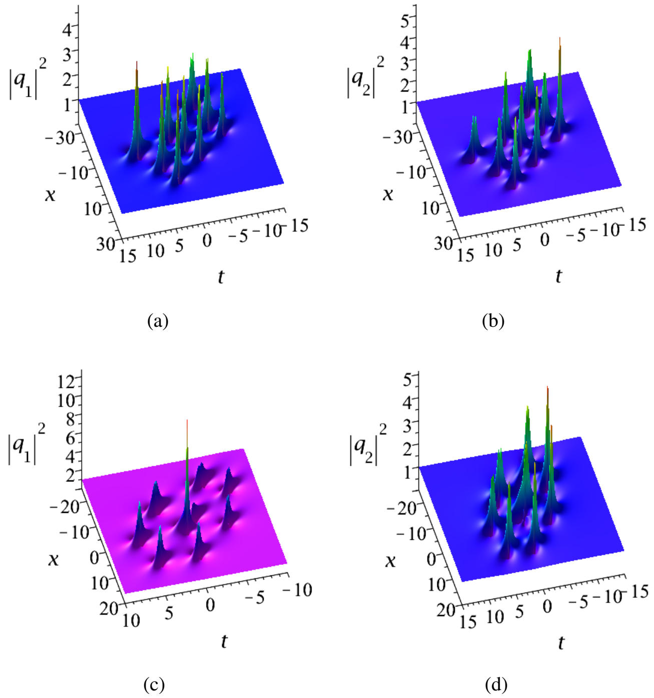

FIGURE 5 The decomposed patterns of the 3rd-order RWs of 2CNLS.

TABLE 2 $\deg(k,n,N)$ of RWs of 3CNLS

k \ n	1	2	3	4	5
0	0	6	18	36	60
1	2	10	24	44	70
2	4	14	30	52	80
3	6	18	36	60	90

On the bases of Tables 1 and 2, we claim a conjecture of $\deg(k,n,N)$ for NCNLS as stated below.

Conjecture 1. The degree of an nth-order rational solution of NCNLS is

$$\deg(k,n,N) = n(n-1)N + 2nk, \quad (k = 0,1,2,3,\cdots,N), \tag{58}$$

and the profiles of RWs can be completely decomposed into individual 1st-order RW peaks with the following number

$$\text{Peak}(k,n,N) = \frac{1}{2}\deg(k,n,N) = \frac{n(n-1)}{2}N + nk. \tag{59}$$

Obviously, Eq. (59) in Conjecture 1 has been revalidated in the case of 2nd-order rational solutions of 3CNLS[60]. Furthermore, the nth-order rational solutions generated by $\boldsymbol{g}_N$ have the equal degree of the $(n+1)$th-order rational solutions generated by $\boldsymbol{g}_0$. Since Eq. (58), it meets,

$$\deg(N,n,N) = n(n-1)N + 2nN = n(n+1)N = \deg(0,n+1,N). \tag{60}$$

It is important to note that $(n+1)$th-order RW with $k=0$ can usually be omitted and replaced by the nth-order RW with $k=N$.

Actually, in recent years, many researchers studied the degree of the polynomial in the rational solutions of the AKNS system. Table 1 in Refs. [41, 43], especially, provided the degree formula of RWs of NLS, which shows $\deg(1,n,1) = n(n+1)$. To complete the tabulation in the case of $k=0$ for NLS, this can be achieved easily:
Perceptibly, Table 3, is the special case of Eq. (58) at $N=1$.

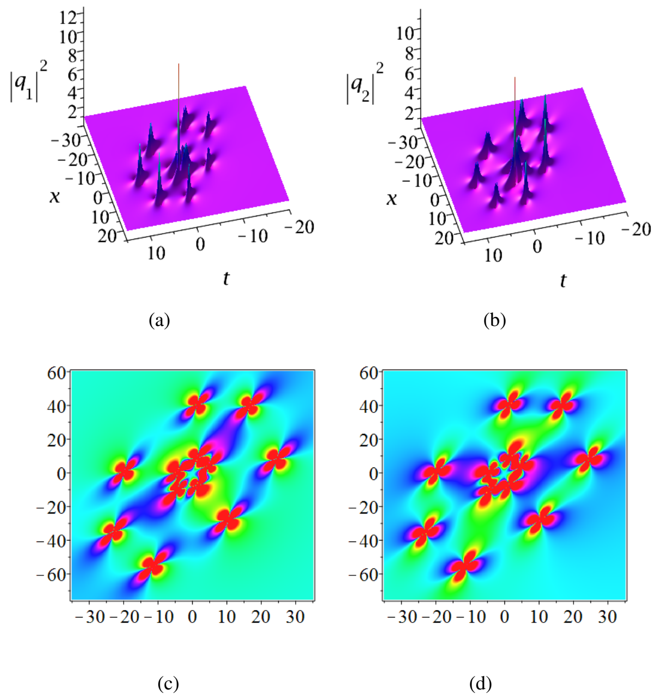

FIGURE 6 The doubly decomposed patterns of 3rd-order RWs of 2CNLS.

TABLE 3 deg (k, n, N) of RWs of NLS

k \ n	1	2	3	4	5	n
0	0	2	6	12	20	$n(n-1)$
1	2	6	12	20	30	$n(n+1)$

In addition, for the circular pattern of the nth-order RW of NLS (viz. $N = 1$ and $k = 1$), it has a circumjacent ring with $2n-1$ peaks and a $(n-2)$th-order RW inside[34, 48, 49]. However, the order of inside RW of the circular pattern is no longer true when $N \geqslant 2$. Since the central peak number $\Delta^1(k, n, N)$, except a single outmost ring of the circular pattern, satisfies

$$\begin{aligned}\Delta^1(k,n,N) &= \text{Peak}\,(k,n,N) - \big((N+1)(n-1)+1\big)\\ &= \frac{(n-1)(n-2)}{2}N + (n-1)k + (k-n), (1 \leqslant k \leqslant N)\end{aligned} \tag{61}$$

which is the peak number of the completely decomposed pattern of inside RW of the circular pattern. Indeed, for NLS[34, 48, 49], $\Delta^1(1, n, 1) = \text{Peak}\,(1, n-2, 1)$, while for $k = n$, $\Delta^1(n, n, N) = \text{Peak}\,(n, n-1, N)$, which is different to the so-called "$(n-2)$th-order" decomposition law of NLS, e.g. Fig. 4(c) and 4(d). In fact, in Figs. 5(c) and 5(d), it shows $\Delta^1(1, 3, 2) = \text{Peak}\,(2, 1, 2)$ for the decomposed case and in Fig. 6 there is even no low order RW of 2CNLS corresponding to the inside pattern.

7 | CHARACTERISTICS OF RWS TO NCMKDV

In this section, high-order flow of multi-component AKNS hierarchy will be introduced and the characteristics of its RWs will be discussed in brief.

In accordance with the compatibility condition, Eq. (58) is also suitable for the rational solutions of the high-order flow of multi-component AKNS hierarchy with the complementary restriction of Eq. (6). A similar analysis would be the 3rd-order flow of a multi-component AKNS system, also known as the N-component complex modified Korteweg-de Vries equation

(NCmKdV), which means $m = 3$ in Eq. (3) and that the matrix $\boldsymbol{N}$ in Eq. (3) evolves into

$$\boldsymbol{N} = 4\lambda^3\boldsymbol{A} + 4\lambda^2\boldsymbol{B} + 2\lambda\boldsymbol{A}(\boldsymbol{B}^2 - \boldsymbol{B}_x) + 2\boldsymbol{B}^3 - \boldsymbol{B}_{xx} + [\boldsymbol{B}_x, \boldsymbol{B}], \tag{62}$$

whilst $\boldsymbol{M}$ is not changed as the matrix given in Eq. (4) for NCNLS. Thus, NCmKdV evolves into

$$q_{j,t} + q_{j,xxx} - 3(q_j\boldsymbol{q})_x\boldsymbol{r} = 0, (j = 1, 2, \cdots, N), \tag{63}$$

and b_j of Eq. (10) in "seed" solution (9) also evolves into

$$b_j = a_j^3 - 3a_jc^2 - 3a_kc_k^2,$$

where, $a_kc_k^2 \triangleq \sum_{k=1}^N a_kc_k^2$, and $c^2 = c_kc_k \triangleq \sum_{k=1}^N c_k^2$.

Under the gauge transformation (23), the matrix (25) evolves into

$$\boldsymbol{N}_0 = -\widetilde{\boldsymbol{M}}_0^3 + 3\mathbf{i}\lambda\widetilde{\boldsymbol{M}}_0^2 + 3\left(\lambda^2 - c^2\right)\widetilde{\boldsymbol{M}}_0 + \mathbf{i}\left(3\left(\lambda^3 + c^2\lambda - a_kc_k^2\right) + n_0\right)\boldsymbol{I}_N. \tag{64}$$

and, the eigenvalue of matrix (64) evolves into

$$\omega_j = -\widetilde{\kappa}_j^3 + 3\mathbf{i}\lambda\widetilde{\kappa}_j^{\,2} + 3\left(\lambda^2 - c^2\right)\widetilde{\kappa}_j + \mathbf{i}\left(3\left(\lambda^3 + c^2\lambda - a_kc_k^2\right) + n_0\right). \tag{65}$$

Then, using (65) instead of (27) to update the diagonal matrix $\boldsymbol{\Lambda}$ in the vector eigenfunction (29), the nth-order solutions to NCmKdV can be obtained by (20).

Next, according to the Eqs. (31)-(34), and the other rest conditions $\sigma_j = 0$, the critical conditions for rational solutions of NCmKdV can also be achieved, such as Eq. (35), (36) for $N = 2$, and Eq. (56) for $N = 3$. Finally, using fundamental vector functions, e.g. Eq. (47) for $N = 2$ and Eq. (57) for $N = 3$, the rational solutions of NCmKdV can be acquired by Eq. (54), which leads identically to the results as Table 1 and Table 2 in the cases of $N = 2$ and $N = 3$, respectively. There are several representative samples shown in Figs. 7 and 8 for $N = 3$.

The circular patterns of the 2nd-order RWs of 3CmKdV with $a_1 = 3/2, c_1 = 1/2, s_1 = 10^4$ are shown in Fig. 7. The figures in each row are all component profiles generated by the fundamental eigenfunctions $\boldsymbol{g}_k$ with $k = 1, 2, 3$ from top to bottom. The circular patterns have one 5-peak ring outside while 2 peaks inside in the case of $k = 2$ and 4 peaks inside in the case of $k = 3$.

The decomposed patterns of the 3rd-order RWs of 3CmKdV generated by fundamental eigenfunction $\boldsymbol{g}_1$ with $a_1 = 3/2, c_1 = 1/2$ are shown in Fig. 8. There are two 5-peak rings outside and 2 peaks inside patterns with $s_1 = 10^5$ in the top row, while one 9-peak ring outside and 3 peaks inside patterns with $s_2 = 10^8$ in the bottom row.

As Figs. 7 and 8 shown above, even for NCmKdV, one $((N+1)(n-1)+1)$-peak ring outside and two $((N+1)(n-2)+1)$-peak rings outside can also be found. This distribution is same as the Figs. 4 - 6 for the NCNLS.

8 | DISCUSSION

In this paper, we only focus on the rational solution of multi-component AKNS with reduction condition (6), which meet the one and only null eigenvalue with multiplicity $N + 1$. In this case, all eigenvalues approach to one critical value λ_0, i.e., $\lambda_j \to \lambda_0\,(j = 1, 2, \cdots, n)$, which is called the full degeneration of n-fold DT. However, we can consider another possibility to obtain semi-rational solutions[35] including combinations of RWs, breathers and solitons. The combinations of RWs and breathers can be generated by partial degenration of n-fold DT from a plane wave "seed" solution $q^{[0]}$, i.e., $\lambda_j \to \lambda_0\,(j = 1, 2, \cdots, k; k < n)$, which can yield kth-order RWs and $(n-k)$th-order breathers. In particular, set $c_j = 0\,(j = k+1, k+2, \cdots, n)$, then the above partial degeneration n-fold DT can generate a semi-rational solution including kth-order RWs and $(n-k)$th-order solitons. In other words, the distinct eigenvalues of Eq. (26) have strong independence in the partial degeneration DT: null eigenvalues lead to the rational solutions parts while non-zero eigenvalues lead to the solitons or breathers parts in a solution. This also means that RWs and solitons or breathers can coexist or be superposed in a semi-rational solution (see the three examples illustrated in **Appendix** B).

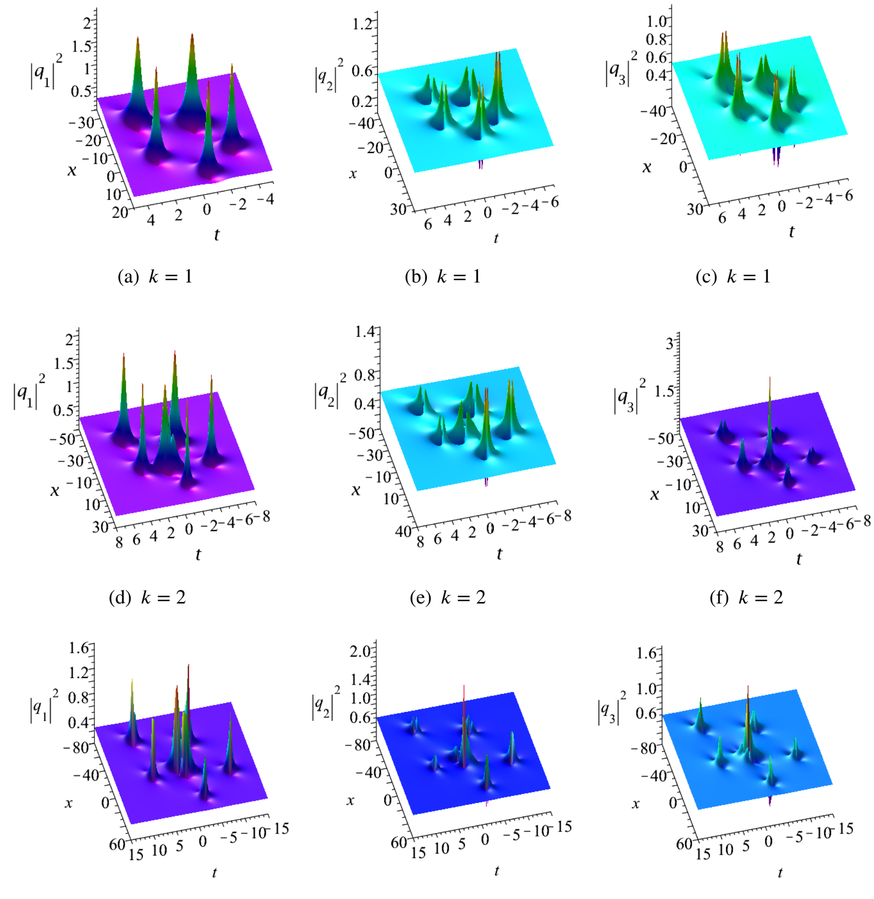

(a) $k = 1$ (b) $k = 1$ (c) $k = 1$

(d) $k = 2$ (e) $k = 2$ (f) $k = 2$

(g) $k = 3$ (h) $k = 3$ (i) $k = 3$

FIGURE 7 The circular patterns of the 2nd-order RWs of 3CmKdV.

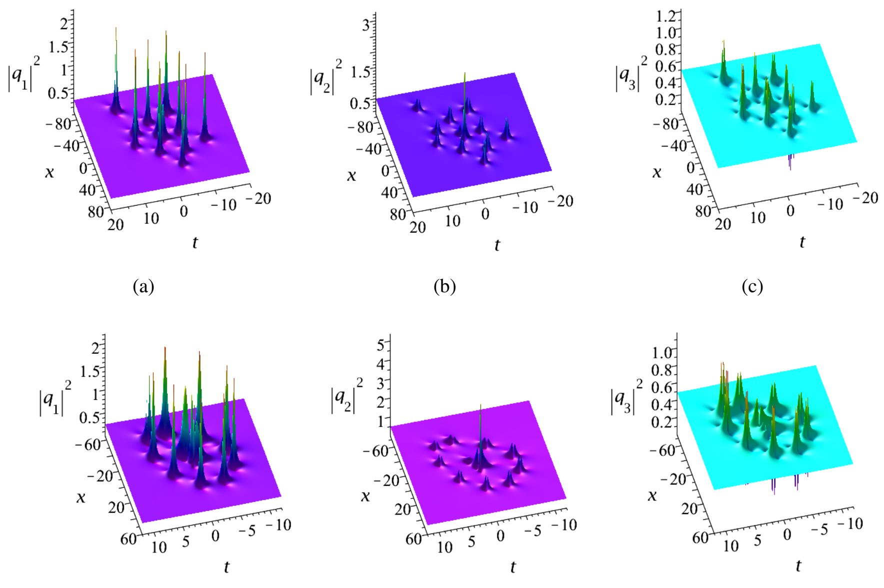

(a) (b) (c)

(d) (e) (f)

FIGURE 8 The decomposed pattern of the 3rd-order RWs of 3CmKdV.

9 | CONCLUSIONS

The multi-component AKNS hierarchy with the complementary restriction (6) leads to an important class of nonlinear integrable equations, for instance NCNLS and NCmKdV, which are used as governing equations in e.g. fluids, Bose-Einstein condensates, plasmas and optics to explain the RW phenomena by the rational solutions [5–14]. This generalization has been revisited recently by e.g. Refs. [30, 50] and further studies about the generating mechanism are discussed in e.g. Refs. [34, 35, 59].

In this paper, we constructed a degenerate n-fold DT to obtain the rational solutions of the two- and three-component NLS equation, respectively, which also hold for the two- and three-component mKdV equation.

To construct the rational solutions, the following specific scheme is proposed.

- First, based on the "seed" solution of Eq. (9), an invertible transformation matrix $\boldsymbol{T}_0$ in Eq. (23) is introduced with two parameters m_0, n_0 to translate the eigenvalues to naught. The associated Lax matrices $\boldsymbol{M}_0$ and N_0 become nilpotent matrices corresponding to the proper values of m_0 and n_0, that is a crucial step to determine polynomial eigenfunctions.
- Second, critical condition for rational solutions is proposed by Eq. (30). From there, the critical value λ_0 of the non-real spectrum parameter λ is acquired and a vector eigenfunction with polynomial entries can be constructed.
- Third, based on the perturbation method, a family of the series multisections $\{\boldsymbol{g}_0, \boldsymbol{g}_1, \cdots, \boldsymbol{g}_N\}$ of vector eigenfunctions are obtained in Eq. (44) as the fundamental eigenfunctions to generate the nth-order rational solutions.
- Finally, the degenerate n-fold DT is constructed by Eq. (54). Using the fundamental eigenfunctions, a complete classification of rational solutions is acquired depending on the exponential threshold k (see Tables 1 and 2).

Consequently, a conjecture about the degree of the nth-order RW in each classification generated by $\boldsymbol{g}_k$ via the n-fold degenerate DT is summed up:

$$\deg(k, n, N) = n(n-1)N + 2nk, \quad (k = 0, 1, 2, 3, \cdots, N).$$

This formula has generalized the result in previous works, e.g. Ref. [43], which shows that $\deg(1, n, 1) = n(n+1)$ for rational solutions of NLS, and implies that RWs with completely decomposed patterns possess $(n(n-1)N/2 + nk)$ 1st-order RW peaks in a local space-time. Furthermore, the circular patterns with one $((N+1)(n-1)+1)$-peak ring outside and with two $((N+1)(n-2)+1)$-peak rings outside are both presented for the NCNLS and NCmKdV cases. Several new patterns of RWs and semi-rational solutions are given in Figs. 5-8 and B1-B3 by multi-fold degenerate DT.

In summary, these results imply that multi-component AKNS hierarchy possesses more abundant dynamical behaviors than the scalar case, which further help us to explore different dynamics in diverse fields such as Bose-Einstein condensates, optical fibers and super-fluids, etc.

ACKNOWLEDGMENTS

This work is supported by the National Natural Science Foundation of China (Grants 11671219 and 12071304) and the Natural Science Foundation of Zhejiang Province (Grant LSY19A010002). Lihong Wang thanks the support by China Scholarship Council (CSC201708330432). Róbert Erdélyi acknowledges the support from the Chinese Academy of Sciences President's International Fellowship Initiative (PIFI, Grant number 2019VMA0052) and is grateful to STFC (UK, Grant number ST/M000826/1) and to The Royal Society (Grant number IE161153). All authors also thank for the advices received from Prof. M.S. Ruderman (University of Sheffield, UK) and Dr. Lijuan Guo (Nanjing Forestry University, University of Science and Technology of China, China).

References

1. Akhmediev N., Ankiewicz A., Taki M.: Waves that appear from nowhere and disappear without a trace. Phys. Lett. A **373**, 675-678 (2009)
DOI: https://doi.org/10.1016/j.physleta.2008.12.036

2. Akhmediev N., Soto-Crespo J. M., and Ankiewicz A.: Extreme waves that appear from nowhere: On the nature of rogue waves. Phys. Lett. A **373**, 2137-2145 (2009)
DOI: https://doi.org/10.1016/j.physleta.2009.04.023

3. Klinting P., Sand S.: Analysis of prototype freak waves. In: R. Darlymple (Ed.) Coastal Hydrodynamics, pp. 618-632. ASCE (1987)
DOI:

4. Dean R. G.: Freak Waves: a Possible Explanation. In: Tørum A., Gudmestad O.T. (eds.) Water Wave Kinematics, pp. 609-612. Springer, Dordrecht (1990)
DOI: https://doi.org/10.1007/978-94-009-0531-3_39

5. Chabchoub A., Hoffmann N. P., Akhmediev N.: Rogue wave observation in a water wave tank. Physical Review Letters **106**, 204502 (2011)
DOI: https://doi.org/10.1103/PhysRevLett.106.204502

6. Chabchoub A., Hoffmann N., Onorato M., Slunyaev A., Sergeeva A., Pelinovsky E., Akhmediev N.: Observation of a hierarchy of up to fifth-order rogue waves in a water tank. Phys. Rev. E. **86**, 056601 (2012)
DOI: https://doi.org/10.1103/PhysRevE.86.056601

7. Bludov Y. V., Konotop V. V., Akhmediev N.: Vector rogue waves in binary mixtures of Bose-Einstein condensates. European Physical Journal Special Topics, **185**, 169-180 (2010)
DOI: https://doi.org/10.1140/epjst/e2010-01247-6

8. Zhao Lichen, Yang Zhanying, Ling Liming, Liu Jie: Precisely controllable bright nonautonomous solitons in Bose-Einstein condensate. Physics Letters A **375**, 1839-1842 (2011)
DOI: https://doi.org/10.1016/j.physleta.2011.03.023

9. Ruderman M. S.: Freak waves in laboratory and space plasmas: Freak waves in plasmas. Eur. Phys. J. Special Topics **185**, 57-66 (2010)
DOI: https://doi.org/10.1140/epjst/e2010-01238-7

10. Bailung H., Sharma S. K., Nakamura Y.: Observation of Peregrine solitons in a multicomponent plasma with negative ions. Physical Review Letters, **107**, 255005 (2011)
DOI: https://doi.org/10.1103/PhysRevLett.107.255005

11. Solli D. R., Ropers C., Koonath P., Jalali B.: Optical rogue waves. Nature (London) **450**, 1054-1058 (2007)
DOI: https://doi.org/10.1038/nature06402

12. Kibler B., Fatome J., Finot C., et al.: The Peregrine soliton in nonlinear fibre optics. Nature Physics **6**, 790-795 (2010)
DOI: https://doi.org/10.1038/nphys1740

13. Dudley J. M., Dias F., Erkintalo M., Genty G.: Instabilities, breathers and rogue waves in optics. Nature Photonics **8**, 755-764 (2014)
DOI: https://dx.doi.org/10.1038/nphoton.2014.220

14. Dudley, J.M., Genty, G., Mussot, A. et al.: Rogue waves and analogies in optics and oceanography. Nature Reviews Physics **1**, 675-689 (2019)
DOI: https://doi.org/10.1038/s42254-019-0100-0

15. Nakamura A., Hirota R.: A New Example of Explode-Decay Solitary Waves in One-Dimension. Journal of the Physical Society of Japan **54**, 491-499 (1985)
DOI: https://doi.org/10.1143/JPSJ.54.491

16. Igor T., Hiroshi T.: Simulation of the ocean waves and appearance of Freak waves. Reports of RIAM Symposium No. 17SP1-2, Proceedings of a symposium held at Chikushi Campus, Kyushu, (2006)
DOI:

17. Akhmediev N. N., Eleonskii V. M., Kulagin N. E.: Exact first-order solutions of the nonlinear Schrödinger equation. Theoretical & Mathematical Physics **72**, 809-818 (1987).
DOI: https://doi.org/10.1007/BF01017105

18. Kuznetsov E. A.: Solitons in Parametrically Unstable Plasma. Soviet Physics Doklady **22**, 507-508 (1977)
DOI:

19. Ma Y.C.: The perturbed plane wave solutions of the cubic nonlinear Schrödinger equation. Studies in Applied Mathematics **60**, 43-58 (1979)
DOI: https://dx.doi.org/10.1002/sapm197960143

20. Peregrine D. H.: Water waves, nonlinear Schrodinger equations and their solutions. J. Austral. Math. Soc. B **25**, 16-43 (1983)
DOI: https://doi.org/10.1017/S0334270000003891

21. Bertola M., Tovbis A.: Universality for the Focusing Nonlinear Schrödinger Equation at the Gradient Catastrophe Point: Rational Breathers and Poles of the Tritronquée Solution to Painlevé I. Communications on Pure and Applied Mathematics **66**, 678-752 (2013)
DOI: https://doi.org/10.1002/cpa.21445

22. Kharif C., Pelinovsky E.: Physical mechanisms of the rogue wave phenomenon. European Journal of Mechanics B/Fluids **22**, 603-634 (2003)
DOI: https://doi.org/10.1016/j.euromechflu.2003.09.002

23. Pelinovsky E., Talipova T., Kharif C.: Nonlinear dispersive mechanism of the freak wave formation in shallow water. Physica D **147**, 83-94 (2000)
DOI: https://doi.org/10.1016/S0167-2789(00)00149-4

24. Onorato M., Residori S., Bortolozzo U., Montinad A., Arecchi F. T.: Rogue waves and their generating mechanisms in different physical contexts. Phys. Rep. **528**, 47-89 (2013)
DOI: https://doi.org/10.1016/j.physrep.2013.03.001

25. Zakharov V. E., Gelash A. A.: Nonlinear Stage of Modulation Instability. Phys. Rev. Lett. **111**, 054101 (2013)
DOI: https://doi.org/10.1103/PhysRevLett.111.054101

26. Biondini G., Mantzavinos D.: Universal Nature of the Nonlinear Stage of Modulational Instability. Phys. Rev. Lett. **116**, 043902 (2016)
DOI: https://doi.org/10.1103/PhysRevLett.116.043902

27. Biondini G., Mantzavinos D.: Long-Time Asymptotics for the Focusing Nonlinear Schrödinger Equation with Nonzero Boundary Conditions at Infinity and Asymptotic Stage of Modulational Instability. Communications on Pure and Applied Mathematics **70**,2300-2365 (2017)
DOI: https://doi.org/10.1002/cpa.21701

28. Adrien E. Kraych, Pierre Suret, Gennady El, Stéphane Randoux.: Nonlinear Evolution of the Locally Induced Modulational Instability in Fiber Optics. Physical Review Letters, **122**, 054101 (2019)
DOI: https://doi.org/10.1103/PhysRevLett.122.054101

29. Bilman D., Miller Peter. D.: A robust inverse scattering transform for the focusing nonlinear Schrödinger equation. Communications on Pure and Applied Mathematics **72**, 1722-1805 (2019)
DOI: https://doi.org/10.1002/cpa.21819

30. Bilman D., Ling L.M., Miller Peter D.: Extreme superposition: Rogue waves of infinite order and the Painlevé-III hierarchy. Duke Mathematical Journal, advance publication, (2020) (also see arXiv:1806.00545v1)
DOI: https://doi.org/10.1215/00127094-2019-0066

31. Ablowitz M. J., Satsuma J.: Solitons and rational solutions of nonlinear evolution equations. J. Math. Phys. **19**, 2180-2186 (1978)
DOI: https://doi.org/10.1063/1.523550

32. Ohta Y., Yang J.K.: General high-order rogue waves and their dynamics in the nonlinear Schrödinger equation. Proc. R. Soc. A **468**, 1716-1740 (2012)
DOI: https://doi.org/10.1098/rspa.2011.0640

33. Matveev V. B.: Some comments on the rational solutions of the Zakharov-Schabat equations. Letters in Mathematical Physics **3**, 503-512 (1979)
DOI: https://doi.org/10.1007/BF00401932

34. He Jingsong, Zhang Hongrui, Wang Lihong, Porsezian K, Fokas A S.: Generating mechanism for higher-order rogue waves. Phys. Rev. E **87**, 052914 (2013)
DOI: https://doi.org/10.1103/PhysRevE.87.052914

35. Degasperis A, Lombardo S.: Rational solitons of wave resonant-interaction models. Physical Review E **88**, 052914 (2013)
DOI: https://doi.org/10.1103/PhysRevE.88.052914

36. Wang Lihong, He Jingsong, Xu Hui, et al.: Generation of higher-order rogue waves from multibreathers by double degeneracy in an optical fiber. Phys. Rev. E **95**, 042217 (2017)
DOI: https://doi.org/10.1103/PhysRevE.95.042217

37. Matveev V. B, Salle M. A.: Darboux transformations and solitons. Springer-Verlag, Berlin (1991)
DOI:

38. He Jingsong, Zhang Ling, Cheng Yi, Li Yishen: Determinant representation of Darboux transformation for the AKNS system. Science in China Series A: Mathematics **49**, 1867-1878 (2006)
DOI: https://doi.org/10.1007/s11425-006-2025-1

39. He Jingsong, Wang Lihong, Li Linjing, Porsezian K., Erdelyi R.: Few-cycle optical rogue waves: Complex modified Korteweg-de Vries equation. Phys. Rev. E **89**, 062917 (2014)
DOI: https://doi.org/10.1103/PhysRevE.89.062917

40. Xing Qiuxia, Wang Lihong, Mihalache D., et al.: Construction of rational solutions of the real modified Korteweg-de Vries equation from its periodic solutions, Chaos **27**, 311-390 (2017)
DOI: https://doi.org/10.1063/1.4982721

41. Akhmediev N., Ankiewicz A., Sotocrespo J. M.: Rogue waves and rational solutions of the nonlinear Schrodinger equation. Phys. Rev. E **80**, 026601 (2009)
DOI: https://doi.org/10.1103/PhysRevE.80.026601

42. Smirnov A. O., Matveev V. B.: Some comments on continuous symmetries of AKNS hierarchy equations and their solutions. arXiv:1509.01134, (2015)
DOI: https://arxiv.org/abs/1509.01134v2

43. Ankiewicz A., Clarkson P., Akhmediev N.: Rogue waves, rational solutions, the patterns of their zeros and integral relations. J. Phys. A: Math. Theor. **43**, 122002 (2010)
DOI: https://doi.org/10.1088/1751-8113/43/12/122002

44. Chin S. A., Ashour O. A., Nikolic S. N., Belic M. R.: Maximal intensity higher-order akhmediev breathers of the nonlinear schrödinger equation and their systematic generation. Physics Letters A **380**, 3625-3629 (2016)
DOI: https://doi.org/10.1016/j.physleta.2016.08.038

45. Gaillard P.: Other $2N-2$ parameters solutions of the NLS equation and $2N+1$ highest amplitude of the modulus of the Nth order AP breather, J. Phys. A, Math. Theor. **48**, 145203 (2015)
DOI: https://doi.org/10.1088/1751-8113/48/14/145203

46. Wang Lihong, Yang Chenghao, Wang Ji, He Jingsong: The height of an nth-order fundamental rogue wave for the nonlinear Schrödinger equation. Physics Letters A **381**, 1714-1718 (2017)
DOI: http://dx.doi.org/10.1016/j.physleta.2017.03.023

47. Dubard P., Matveev V B.: Multi-rogue waves solutions: from the NLS to the KP-I equation. Nonlinearity **26**, R93-R125 (2013)
DOI: https://doi.org/10.1088/0951-7715/26/12/R93

48. Kedziora D. J., Ankiewicz A. and Akhmediev N.: Classifying the hierarchy of nonlinear-Schrödinger-equation rogue-wave solutions. Phys. Rev. E **88**, 013207 (2013)
DOI: https://doi.org/10.1103/PhysRevE.88.013207

49. Wang Lihong, Porsezian K, He Jingsong: Breather and rogue wave solutions of a generalized nonlinear Schrödinger equation. Phys. Rev. E **87**, 053202 (2013)
DOI: https://doi.org/10.1103/PhysRevE.87.053202

50. Ling Liming and Zhao Lichen: Simple determinant representation for rogue waves of the nonlinear Schrodinger equation. Phys. Rev. E **88**, 043201 (2013)
DOI: https://doi.org/10.1103/PhysRevE.88.043201

51. Kedziora D. J., Ankiewicz A., Akhmediev N.: Triangular rogue wave cascades. Phys. Rev. E **86**, 056602 (2012)
DOI: https://doi.org/10.1103/PhysRevE.86.056602

52. Kedziora D. J., Ankiewicz A., and Akhmediev N.: Circular rogue wave cluster. Phys. Rev. E **84**, 056611 (2011)
DOI: https://doi.org/10.1103/PhysRevE.84.056611

53. Manakov S. V.: On the theory of two-dimensional stationary self-focusing of electromagnetic waves. Soviet Journal of Experimental and Theoretical Physics **38**, 248-253 (1974)
DOI:

54. Wright O. C., Forest M. G.: On the Bäcklund-gauge transformation and homoclinic orbits of a coupled nonlinear Schrödinger system. Physica D-nonlinear Phenomena **141**, 104-116 (2000)
DOI: https://doi.org/10.1016/S0167-2789(00)00021-X

55. Wright O. C.: The Darboux transformation of some Manakov systems. Applied Mathematics Letters **16**, 647-652 (2003)
DOI: https://doi.org/10.1016/S0893-9659(03)00061-2

56. He Jingsong, Guo Lijuan, Zhang Yongshuai, Chabchoub A.: Theoretical and experimental evidence of non-symmetric doubly localized rogue waves. Proc. R. Soc. A **470**, 20140318 (2014)
DOI: https://doi.org/10.1098/rspa.2014.0318

57. Ling Liming, Guo Boling, Zhao Lichen: High-order rogue waves in vector nonlinear Schrodinger equations. Phys. Rev. E **89**, 041201 (2014)
DOI: https://doi.org/10.1103/PhysRevE.89.041201

58. Zhao Lichen, Guo Boling, Ling Liming: High-order rogue wave solutions for the coupled nonlinear Schroinger equations-II. J. Math. Phys. **57**, 043508 (2016)
DOI: https://doi.org/10.1063/1.4947113

59. Baronio F., Degasperis A., Conforti M., et al.: Solutions of the vector nonlinear Schrödinger equations: evidence for deterministic rogue waves. Physical Review Letters **109**, 044102 (2012)
DOI: https://doi.org/10.1103/PhysRevLett.109.044102

60. Zhang Guoqiang, Yan Zhenya: Three-component nonlinear Schrödinger equations: modulational instability, Nth-order vector rational and semi-rational rogue waves, and dynamics. Communications in Nonlinear Science and Numerical Simulation **62**, 117-133 (2018)
DOI: https://doi.org/10.1016/j.cnsns.2018.02.008

61. Zhao Lichen, Liu Jie: Rogue-wave solutions of a three-component coupled nonlinear Schrödinger equation. Physical Review E **87**, 013201 (2013)
DOI: https://doi.org/10.1103/PhysRevE.87.013201

62. Biondini G., Kraus D. K., Prinari B.: The three-component defocusing nonlinear Schrödinger equation with nonzero boundary conditions. Communications in Mathematical Physics **348**, 475-533 (2016)
DOI: https://doi.org/10.1007/s00220-016-2626-7

63. Ablowitz M. J., Clarkson P. A.: Solitons, nonlinear evolution equations and inverse scattering. Cambridge University Press, Cambridge (1991)
DOI: https://doi.org/10.1017/CBO9780511623998

64. Riordan J.: Combinatorial identities, pp. 131-141. John Wiley and Sons, New York (1968)
DOI:

$\square$

APPENDIX

A NUMERATOR AND DENOMINATOR OF $\boldsymbol{B}_1'$

In this appendix, the denominator of $\boldsymbol{B}_1'$ is shown for the 2nd-order RWs of NCNLS. further, two numerators in $\boldsymbol{B}_1'$ for the 2nd-order RWs of 2CNLS are also listed below.

Based on Eq. (54), the denominator of $\boldsymbol{B}_1'$ for the 2nd-order RWs of NCNLS can be obtained by the Cramer's rule:

$$\left(v_{1,k}^*\right)^2 c_1 \left(\left(\sum_{j=1}^{N+1} |v_{j,k}|^2 \right)^2 c_1^2 - (\lambda_0^* - \lambda_0)^2 \sum_{i=1}^{N} \sum_{j=i+1}^{N+1} |v_{i,k} v_{j,k+N+1} - v_{i,k+N+1} v_{j,k}|^2 \right), \tag{A1}$$

of which $k = 0, 1, \cdots, N$, and

$$-(\lambda_0^* - \lambda_0)^2 = 4 \operatorname{Im}\left(\lambda_0\right)^2 > 0.$$

Two numerators in $\boldsymbol{B}_1'$ for the 2nd-order RWs of 2CNLS are expressed by the Taylor coefficients $\boldsymbol{v}_k$ and $\boldsymbol{v}_{k+N+1}$ of $\boldsymbol{g}_k$ in Eq. (45). The expression of the numerators are listed below.

The numerator of the 1st component of $\boldsymbol{q}_{\mathrm{rw}}^{[2]}$ to 2CNLS reads as

$$(v_{1,k}^*)^2 c_1 (\lambda_0^* - \lambda_0) \left(2 v_{2,k}^* v_{1,k} \left(\sum_{j=1}^{N+1} |v_{j,k}|^2 \right) c_1^2 + (\lambda_0^* - \lambda_0) F_1 c_1 - (\lambda_0^* - \lambda_0)^2 F_2 \right), \tag{A2}$$

of which

$$\begin{aligned} F_1 = {} & (v_{2,k}^*)^2 (v_{1,k} v_{2,k+3} - v_{2,k} v_{1,k+3}) + v_{2,k}^* v_{3,k}^* (v_{1,k} v_{3,k+3} - v_{3,k} v_{1,k+3}) + \\ & v_{1,k}^2 (v_{1,k} v_{2,k+3} - v_{2,k} v_{1,k+3})^* - v_{1,k} v_{3,k} (v_{2,k} v_{3,k+3} - v_{3,k} v_{2,k+3})^*, \end{aligned}$$

and

$$F_2 = (v_{1,k} v_{3,k+3} - v_{3,k} v_{1,k+3})(v_{2,k} v_{3,k+3} - v_{3,k} v_{2,k+3})^*.$$

The numerator of the the 2nd component is

$$-(v_{1,k}^*)^2 c_1 (\lambda_0^* - \lambda_0) \left(2 v_{3,k}^* v_{1,k} \left(\sum_{j=1}^{N+1} |v_{j,k}|^2 \right) c_1^2 + (\lambda_0^* - \lambda_0) G_1 c_1 + (\lambda_0^* - \lambda_0)^2 G_2 \right), \tag{A3}$$

of which

$$\begin{aligned} G_1 = {} & (v_{3,k}^*)^2 (v_{1,k} v_{3,k+3} - v_{3,k} v_{1,k+3}) + v_{2,k}^* v_{3,k}^* (v_{1,k} v_{2,k+3} - v_{2,k} v_{1,k+3}) + \\ & v_{1,k}^2 (v_{1,k} v_{3,k+3} - v_{3,k} v_{1,k+3})^* + v_{1,k} v_{2,k} (v_{2,k} v_{3,k+3} - v_{3,k} v_{2,k+3})^*, \end{aligned}$$

and

$$G_2 = (v_{1,k} v_{2,k+3} - v_{2,k} v_{1,k+3})(v_{2,k} v_{3,k+3} - v_{3,k} v_{2,k+3})^*.$$

B SEMI-RATIONAL SOLUTION

In 2CNLS, i.e. the simplest example of the multi-component NLS, semi-rational solutions have be derived in Ref. [35] with the superposition of the same order soliton (breather) and RW. In this paper, the semi-rational solutions of 2CNLS with the coexistence patterns of different order soliton (breather) and RW will be shown in Figs. B1-B3. The semi-rational solution construction method is described briefly in **Appendix** C.

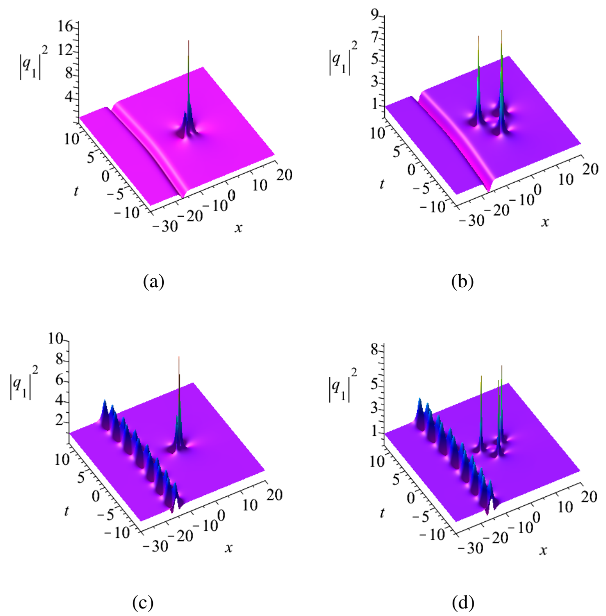

FIGURE B1 Profile of $|q_1|^2$ of semi-rational solution with one- soliton/breather mixed with a 2nd-order RW patterns. There are one-soliton and 2nd-order RWs mixed in the top row, while one-breaher and 2nd-order RWs are mixed in the bottom row. The 2nd-order RWs in the left column are visualising the fundamental patterns, while on the right there are the triangle patterns. The corresponding parameters are $a_1 = 0, c_1 = 1, u_0 = 0, v_1 = 1, \boldsymbol{v} = -10$ in all figures and (a) $u_1 = 0, c_2 = 0$, (b) $u_1 = 100, c_2 = 0$, (c) $u_1 = 0, c_2 = 1$, (d) $u_1 = 100, c_2 = 1$, respectively.

In Fig. B1, the coexistence patterns of 2nd-order RWs mixed with one-soliton or one-breather are shown to illustrate that the nonzero eigenvalue of Eq. (26) can lead to a soliton and a breather. In Fig. B2, the coexistence patterns of 3rd-order RWs mixed with one- or two- soliton are shown to illustrate the 3rd-order RWs can possess independently all patterns (fundamental and decomposed) whatever the order of the mixed solitons. In Fig. B3, the coexistence patterns of 4th-order RWs mixed with one-soliton are shown to illustrate the completely decomposed patterns are also valid in the semi-rational solution.

Based on Figs. B1-B3 illustrated above, the RW and soliton (breather) can be separated from each other, while the RW and soliton (breather) are far enough away. Thus, we focus merely on the case with less components for rational solutions instead of semi-rational solutions in this paper. Another aspect is that, the more components the more combinations. In fact, when the number of components $N \geqslant 4$, this will give rise to the problem of the expression of the root formulas of a quintic characteristic polynomial or higher degree polynomial which will be discussed in a further paper.

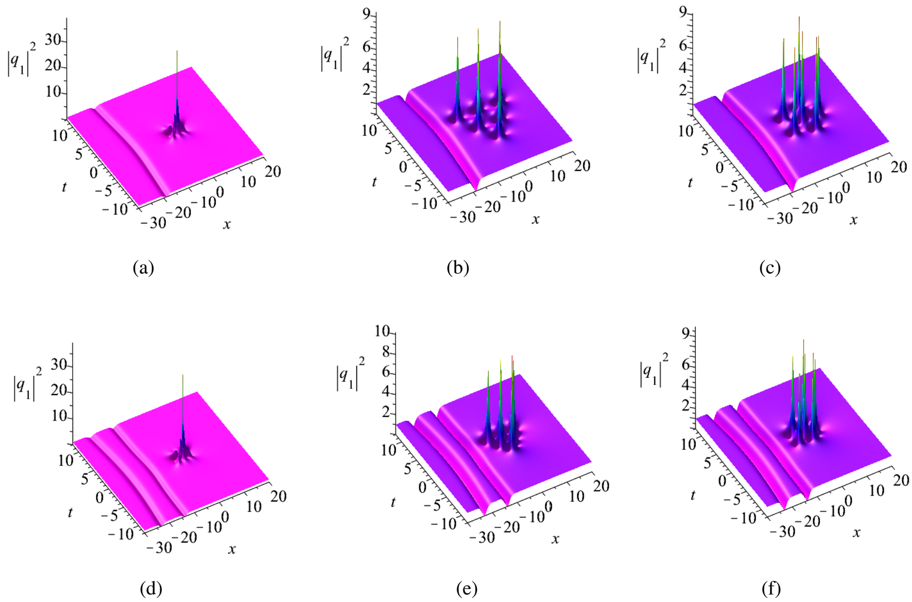

FIGURE B2 Profile of $|q_1|^2$ of semi-rational solution with one- and two- soliton mixed with 3rd-order RW patterns. There are one-soliton shown in the top row and two-soliton shown in the bottom row. The 3rd-order RWs are fundamental, triangle and circular patterns, respectively, from left to right. The corresponding parameters are $a_1 = a_2 = 0, c_1 = 1, c_2 = 0, u_0 = 0, \boldsymbol{v} = -10$ and the others are (a) $u_1 = 0, u_2 = 0, v_2 = 1$, (b) $u_1 = 100, u_2 = 0, v_2 = 1$, (c) $u_1 = 0, u_2 = 1000, v_2 = 1$, (d) $u_1 = 0, u_2 = 0, v_1 = 1$, (e) $u_1 = 20, u_2 = 0, v_1 = 1$, (f) $u_1 = 0, u_2 = 100, v_1 = 1$, respectively.

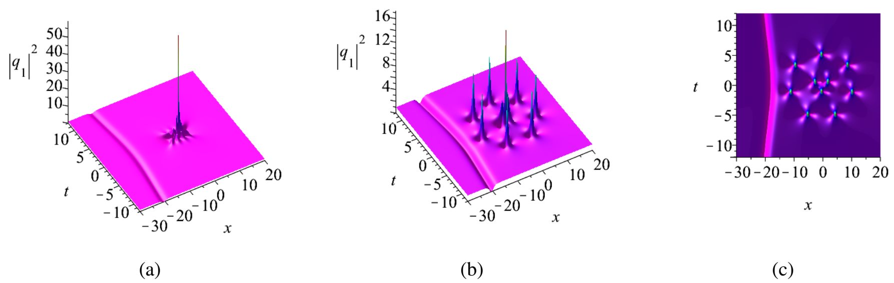

FIGURE B3 Profile of $|q_1|^2$ of semi-rational solution with one-soliton mixed with the 4th-order RW pattern. The 4th-order RWs are fundamental, circular (7-peak ring outside and a 2nd-oder fundamental pattern inside), and completely decomposed pattern (7-peak ring outside and a 2nd-order triangle pattern inside) from left to right. The corresponding parameters are $a_1 = a_2 = 0, c_1 = 1, c_2 = 0, u_0 = 0, u_2 = 0, v_3 = 1, \boldsymbol{v} = -10$ in all figures and (a) $u_1 = 0, u_3 = 0$, (b) $u_1 = 0, u_3 = 10^5$, (c) $u_1 = 10, u_3 = 10^5$, respectively.

C SOLUTION OF 2CNLS

In this appendix, the semi-rational solution of 2CNLS, namely Manakov system, will be derived in brief.

First, let $\sigma_0 = \sigma_1 = 0$ in Eq. (26), and the pseudo-remainder $\widetilde{\sigma}_0$ of polynomials σ_0 and σ_1 in λ satisfies $\widetilde{\sigma}_0 \equiv 0$ for any complex λ (or let the discriminant of Eq. (26) and its leading coefficient in λ vanish) to obtain a double null eigenvalue, it yields

$$a_2 = a_1, m_0 = -\frac{a_1}{2}, \lambda_0 = -\frac{1}{2}a_1 + \mathbf{i}c. \tag{C1}$$

Here, $c = \sqrt{c_1^2 + c_2^2}$. Based on the conditions (C1), $n_0 = -\frac{b_1}{2}$ can also be obtained from the characteristic polynomial of $\boldsymbol{N}_0$ in the same way.

Furthermore, the eigenvalues of $\boldsymbol{M}_0$ can be simplified under the conditions (C1),

$$\kappa_1, \kappa_2, \kappa_3 = \mathbf{i}h, -\mathbf{i}h, \mathbf{i}\left(\lambda + \frac{a_1}{2}\right), \tag{C2}$$

where, $h = \sqrt{\left(\lambda + \frac{a_1}{2}\right)^2 + c^2}$ and the corresponding eigenvalues of $\boldsymbol{N}_0$ are

$$\omega_1, \omega_2, \omega_3 = \mathbf{i}h(2\lambda - a_1), -\mathbf{i}h(2\lambda - a_1), \frac{1}{2}\mathbf{i}(4\lambda^2 + b_1). \tag{C3}$$

Let

$$\boldsymbol{\zeta} = \begin{pmatrix} \exp(\mathbf{i}h\boldsymbol{u}) \\ -\exp(-\mathbf{i}h\boldsymbol{u}) \\ \boldsymbol{\nu}\exp\left(-\mathbf{i}(\lambda + \frac{a_1}{2})\boldsymbol{v}\right)\epsilon \end{pmatrix}, \tag{C4}$$

where

$$\boldsymbol{u} = u_0 + \sum_{k=1}^{N} u_k \epsilon^{2k}, \boldsymbol{v} = v_0 + \sum_{k=1}^{N} v_k \epsilon^{2k}, \boldsymbol{\nu} = \nu_0 + \sum_{k=1}^{N} \nu_k \epsilon^{2k},$$

a vector eigenfunction of system (22) can be obtained

$$\boldsymbol{\varphi} = \boldsymbol{\Phi\Lambda} \begin{pmatrix} \exp(\mathbf{i}h\boldsymbol{u}) \\ -\exp(-\mathbf{i}h\boldsymbol{u}) \\ \boldsymbol{\nu}\exp\left(-\mathbf{i}(\lambda + \frac{a_1}{2})\boldsymbol{v}\right)\epsilon \end{pmatrix}, \tag{C5}$$

where,

$$\boldsymbol{\Phi} = (\boldsymbol{\eta}_1, \boldsymbol{\eta}_2, \boldsymbol{\eta}_3) = \begin{pmatrix} \mathbf{i}(\lambda + \frac{a_1}{2} - h) & \mathbf{i}(\lambda + \frac{a_1}{2} + h) & 0 \\ c_1 & c_1 & -c_2 \\ c_2 & c_2 & c_1 \end{pmatrix}, \tag{C6}$$

and

$$\boldsymbol{\Lambda} = \mathbf{diag}\left(\exp(\vartheta_1), \exp(\vartheta_2), \exp\left(\vartheta_3\right)\right).$$

Here, $\vartheta_1 = \mathbf{i}h(x + (2\lambda - a_1)t), \vartheta_2 = -\vartheta_1$, and $\vartheta_3 = \frac{1}{2}\mathbf{i}\left((2\lambda + a_1)x + (4\lambda^2 + b_1)t\right)$.

When $\boldsymbol{\nu} = 0$, the non-symmetric RWs are discussed in detail in Ref. [56] (namely the case of $\boldsymbol{\zeta} = (K_1, K_2, K_3)^T = (1, -1, 0)^T$ in Ref. [56]), it will not be repeated in this paper.

When $\boldsymbol{\nu} \neq 0$, let $\lambda = \lambda_0 + \epsilon^2$, using $\boldsymbol{\varphi}$ in Eq. (C5) instead of $(f, g, h)^T$ in Ref. [56], then the semi-rational solutions can be obtained by Eq. (3.5) in Ref. [56].